J. Geomag. Geoelectr., **49**, 1469–1497, 1997

Fast and Stable Two-Dimensional Inversion of Magnetotelluric Data

Patricia Pastana DE LUGÃO*, Oleg PORTNIAGUINE, and Michael S. ZHDANOV

Department of Geology and Geophysics, University of Utah, Salt Lake City, UT 84112, U.S.A.

(Received October 18, 1996; Revised July 5, 1997; Accepted August 14, 1997)

The two-dimensional (2-D) magnetotelluric (MT) inverse problem still poses difficult challenges in spite of efforts to develop fast and efficient methods for its solution. In this paper, we present a new approach for the solution of overparameterized cases based on regularization theory and full 2-D, quasi-analytic, calculation of the Frechet derivatives. For the forward solution we use a fast and efficient finite difference formulation to the solution of the MT equations in both transverse electric (TE) and transverse magnetic (TM) modes based on the balance method. The Frechet derivative matrix is obtained as a solution to simple forward and back substitution of the LU decomposed matrix of coefficients from the forward problem utilizing the principle of reciprocity. Magnetotelluric data is usually contaminated by noise, so that its inverse problem is ill-posed. In order to constrain the solution to a set of acceptable models, Tikhonov regularization is applied and yields a regularized parametric functional. The regularized conjugate gradient method is then utilized to minimize the parametric functional. Results of inversion for a set of synthetic data and for a set of CSAMT data from Kennecott Exploration show that the method yields models which are physically and geologically reasonable for both synthetic and real data sets.

1. Introduction

The 2-D MT inverse problem has been addressed by several authors. The most well-known approaches for the solution of overparameterized cases are the search for a smooth model in the Occam code from de Groot-Hedlin and Constable (1990) and the Rapid Relaxation Inverse (RRI) solution of Smith and Booker (1991). The main limitations of these approaches are in the smooth model assumed for the inversion and in the calculation of the Frechet, or sensitivity, matrix. The smooth model is a very artificial approximation to the real model of the earth, which contains sharp boundaries between structures with different conductivities. Also, the RRI method is based on the approximate calculation of the Frechet derivatives under the assumption that horizontal variations in conductivity are much smaller than vertical ones. In real inhomogeneous structures we can observe strong conductivity contrasts both in vertical and in horizontal directions. In the Occam code, the calculation of the Frechet matrix is the most time consuming part of the code.

In this paper we present a different approach dealing with the model of an arbitrary structure containing both smooth subdomains and areas with sharp conductivity contrasts. This approach is based on regularization theory and the fast, full 2-D, quasi-analytic calculation of the Frechet derivatives.

For the forward solution, we use a fast and efficient finite difference formulation to the solution of MT equations in both TE and TM modes based on the balance method of Zhdanov *et al.* (1982), but modified to obtain a symmetric matrix of coefficients. This modification was required in order to apply reciprocity using the methodology described in de Lugão and Wannamaker (1996) for the calculation of the Frechet matrix.

*Now at Western Atlas Logging Services, 10205 Westheimer, Houston, Tx 77042, U.S.A.

The calculation of the Frechet derivative matrix can be one of the most computationally expensive tasks in the solution of an overparameterized inverse problem. In this work, the Frechet derivative matrix is obtained as a solution to simple forward and back substitution of the LU decomposed matrix of coefficients from the forward problem with different right hand terms due to the sources introduced by differentiation of the inversion parameters. Utilizing the principle of reciprocity (Rodi, 1976; Tripp *et al.*, 1984; Sasaki, 1989; de Lugão and Wannamaker, 1996), the number of forward and back substitutions performed decreases from the number of inversion parameters to the number of receivers of interest.

The inverse problem in magnetotellurics is ill-posed since the data is usually contaminated with noise: a solution may not exist or there may be many solutions that fit the data. In the search for a stable solution to the two-dimensional magnetotelluric inverse problem, we apply Tikhonov regularization (Tikhonov and Arsenin, 1977) utilizing a stabilizing functional which ties the solution to an *a priori* model. In order to minimize the parametric functional, we utilize the non-linear conjugate gradient method (Zhdanov, 1993).

We present validation for the forward code and for the calculation of the Frechet terms for apparent resistivity and phase data in both TE and TM modes. Inversion is first performed for separate sets of TE and TM synthetic apparent resistivity and phase data from COMMEMI model 2D-1 (Zhdanov *et al.*, 1990) and the models obtained from inversion are consistent with the resolution of each mode, independently. Results are then presented for inversion of a set of TM mode apparent resistivity and phase CSAMT data from Kennecott Exploration and the model obtained from inversion resolves both known and new resistive targets.

2. 2-D Finite Difference Forward Solution

The forward solution utilized in the inversion was written based on a finite difference scheme formulated by Zhdanov *et al.* (1982). However, the coefficients used in the approximation were rearranged in order to obtain a symmetric matrix of coefficients. The symmetry of the coefficient matrix is a necessary condition in the method used for the calculation of the Frechet derivative matrix and will be discussed in the next section.

We assume time dependence $e^{-i\omega t}$ and neglect displacement currents. In cartesian coordinates, the strike direction is y to the south, x is west-east and z is down.

For the TE mode we solve the Helmholtz equation to obtain the total electric field parallel to strike, E_y:

$$\nabla^2 E_y + \kappa^2 E_y = 0, \tag{1}$$

with components of the auxiliary magnetic field:

$$H_x = -\frac{1}{i\omega\mu_0}\frac{\partial E_y}{\partial z} \tag{2}$$

and

$$H_z = \frac{1}{i\omega\mu_0}\frac{\partial E_y}{\partial x}. \tag{3}$$

For the TM mode the equation to solve for the total magnetic field parallel to strike is:

$$\nabla \cdot \left(\frac{1}{\kappa^2}\nabla H_y\right) + H_y = 0, \tag{4}$$

with components of the auxiliary electric field:

$$E_x = -\frac{1}{\sigma}\frac{\partial H_y}{\partial z} \tag{5}$$

and

$$E_z = \frac{1}{\sigma}\frac{\partial H_y}{\partial x}, \tag{6}$$

where

$$\kappa^2 = i\omega\mu\sigma. \tag{7}$$

Two meshes are constructed. Mesh Σ discretizes the fields parallel to strike $F_y(x_i, z_j)$, where F_y is either E_y in the TE mode or H_y in the TM mode. An auxiliary mesh Σ' is constructed on the nodes placed in the center of the main mesh in order to discretize $\kappa^2(x_{i\pm1/2}, z_{j\pm1/2})$.

In the TE mode, the Laplacian of E_y is approximated by an integral over the rectangular boundary L_{ij} of the cell S_{ij} using Green's theorem:

$$\int_{L_{ij}} \frac{\partial E_y}{\partial n} dl = -\iint_{S_{ij}} \kappa^2 E_y dxdz. \tag{8}$$

In the TM mode, the integral identity resulting from approximation of Eq. (4) is:

$$\int_{L_{ij}} \frac{1}{\kappa^2}\frac{\partial H_y}{\partial n} dl = -\iint_{S_{ij}} H_y dxdz. \tag{9}$$

Evaluating these integrals by the sample values $F_y(i,j)$ and $\kappa^2(i \pm 1/2, j \pm 1/2)$, we arrive at a system of difference equations for the solution of the total fields parallel to strike at the internal nodes of the main mesh Σ:

$$\alpha_{ij}^{(0)} F(i,j) = [\alpha_{ij}^{(1)} F(i+1,j) + \alpha_{ij}^{(2)} F(i,j+1) + \alpha_{ij}^{(3)} F(i-1,j) + \alpha_{ij}^{(4)} F(i,j-1)] \tag{10}$$

where F is E_y in the TE mode and H_y in the TM mode.

For the TE mode the coefficient $\alpha_{ij}^{(0)}$ is a complex constant while $\alpha_{ij}^{(1)}, \alpha_{ij}^{(2)}, \alpha_{ij}^{(3)}, \alpha_{ij}^{(4)}$ are real constants. The indeces i and j range from $i = 2, \ldots, N_I - 1$ and $j = 2, \ldots, N_J - 1$, where N_I and N_J are respectively the total number of horizontal and vertical nodes in the mesh. We then obtain the following coefficients:

$$\alpha_{ij}^{(1)} = \frac{\Delta\tilde{z}_j}{\Delta x_i}, \qquad \alpha_{ij}^{(2)} = \frac{\Delta\tilde{x}_i}{\Delta z_j}, \qquad \alpha_{ij}^{(3)} = \frac{\Delta\tilde{z}_j}{\Delta x_{i-1}}, \qquad \alpha_{ij}^{(4)} = \frac{\Delta\tilde{x}_i}{\Delta z_{j-1}},$$

and

$$\alpha_{ij}^{(0)} = \sum_{\ell=1}^{4} \alpha_{ij}^{(\ell)} - \frac{1}{4}\sum_{p=0}^{1}\sum_{q=0}^{1} \kappa_{ij}^{2pq} S^{pq}, \tag{11}$$

which form a symmetric matrix $\hat{A}_{TE}$.

For the TM mode all coefficients are complex and depend on the conductivity σ. We obtain the following coefficients, which form the symmetric matrix $\hat{A}_{TM}$:

$$\alpha_{ij}^{(1)} = \frac{\sum_{q=0}^{1} \frac{S^{1,q}}{\kappa_{ij}^{21,q}}}{2(\Delta x_i)^2}, \qquad \alpha_{ij}^{(2)} = \frac{\sum_{p=0}^{1} \frac{S^{p,1}}{\kappa_{ij}^{2p,1}}}{2(\Delta z_j)^2},$$

$$\alpha_{ij}^{(3)} = \frac{\sum_{q=0}^{1} \frac{S^{0,q}}{\kappa_{ij}^{20,q}}}{2(\Delta x_{i-1})^2}, \qquad \alpha_{ij}^{(4)} = \frac{\sum_{p=0}^{1} \frac{S^{p,0}}{\kappa_{ij}^{2p,0}}}{2(\Delta z_{z-1})^2},$$

and

$$\alpha_{ij}^{(0)} = \sum_{\ell=1}^{4} \alpha_{ij}^{(\ell)} - S_{ij}, \tag{12}$$

where:

$$\Delta\tilde{x}_i = (\Delta x_{i-1} + \Delta x_i)/2, \qquad \Delta\tilde{z}_j = (\Delta z_{j-1} + \Delta z_j)/2,$$

$$S^{pq} = \Delta x_{i+p-1}\Delta z_{j+q-1}, \qquad S_{ij} = \Delta\tilde{x}_i\Delta\tilde{z}_j,$$

and

$$\kappa_{ij}^{2pq} = \kappa^2(i + p - \frac{1}{2}, j + q - \frac{1}{2}). \tag{13}$$

Using matrix notations we have the following system of equations:

$$\widehat{A} \cdot \hat{F} = \hat{C}^F, \tag{14}$$

where $\hat{F}$ is the vector of unknown values for the E_y or H_y components over mesh Σ, $\hat{A}$ is the matrix of coefficients, $\hat{A}_{TE}$ or $\hat{A}_{TM}$, for the system and $\hat{C}$ is the vector of free terms, in which the only non-zero terms are those at the boundary nodes for mesh Σ.

The structure of matrix $\hat{A}$ essentially depends on the method used in ordering the vector $\hat{F}$ and on the choice of boundary conditions. Here, we solve for total field values at each node inside the mesh and the normal (or 1-D) field values are taken as the boundary condition. The nodes of the mesh are numbered consecutively along the horizontal and vertical.

Matrix $\hat{A}$ is complex, symmetric, penta-diagonal and diagonally dominant. The dimensions of $\hat{A}$ are given by the number of horizontal $N_I - 2$ and vertical $N_J - 2$ internal nodes in the

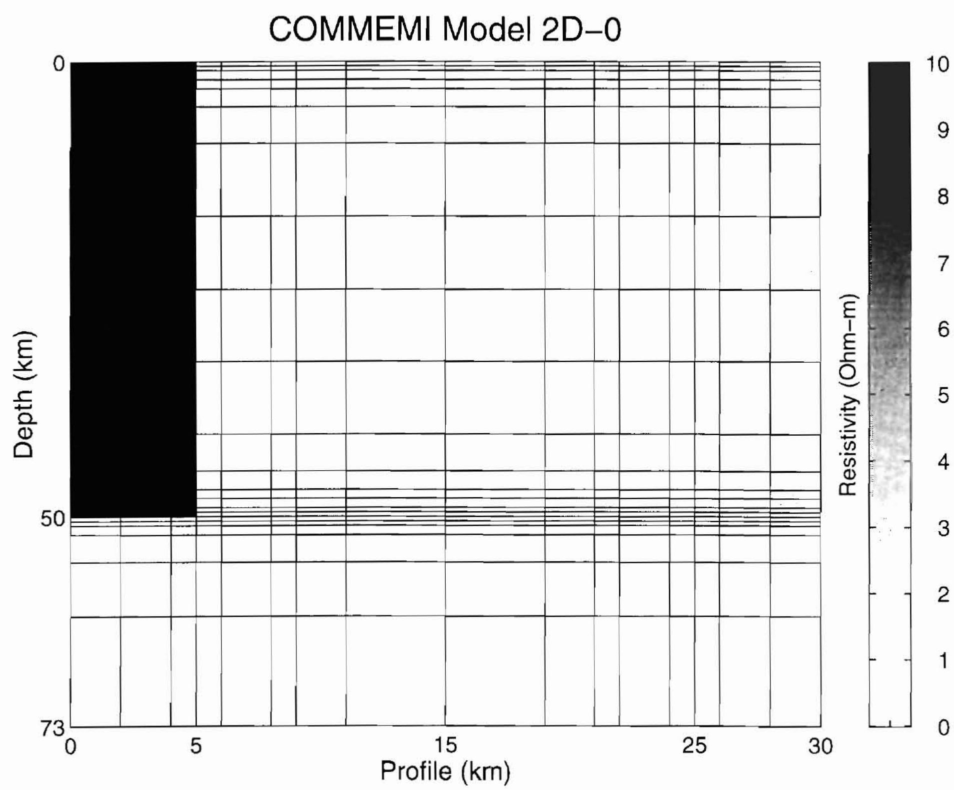

Fig. 1. COMMEMI model 2D-0 used to check forward code and calculations of Frechet matrix with period of 300 s.

mesh. The leading dimension N is given by $(N_I - 2) \times (N_J - 2)$, and the bandwidth is given by $2 \times (N_I - 2) + 1$.

The Crout method is used to decompose matrix $\hat{A}$ in LU form and solve Eq. (14). No pivoting is required due to the fact that $\hat{A}$ is diagonally dominant (Lapidus and Pinder, 1982). The Crout subroutine creates only the five elements of $\hat{A}$ that are needed at each step in decomposing the matrix. The upper and lower diagonal matrices $\hat{L}$ and $\hat{U}$ are also banded, each with bandwidth $(N_I - 2) + 1$. These matrices are then stored since they are needed for calculation of the Frechet derivative matrix.

The choice of a direct method was done with the inversion scheme in mind. The calculation of the Frechet matrix will be performed in a quasi-analytic manner, utilizing the LU decomposed matrix of coefficients. The LU decomposition is the most computationally demanding task in the code, requiring about $(N^3)/3$ computations in its primitive form. In our algorithm, the Crout scheme used takes into consideration the banded structure of the matrix, decreasing the number

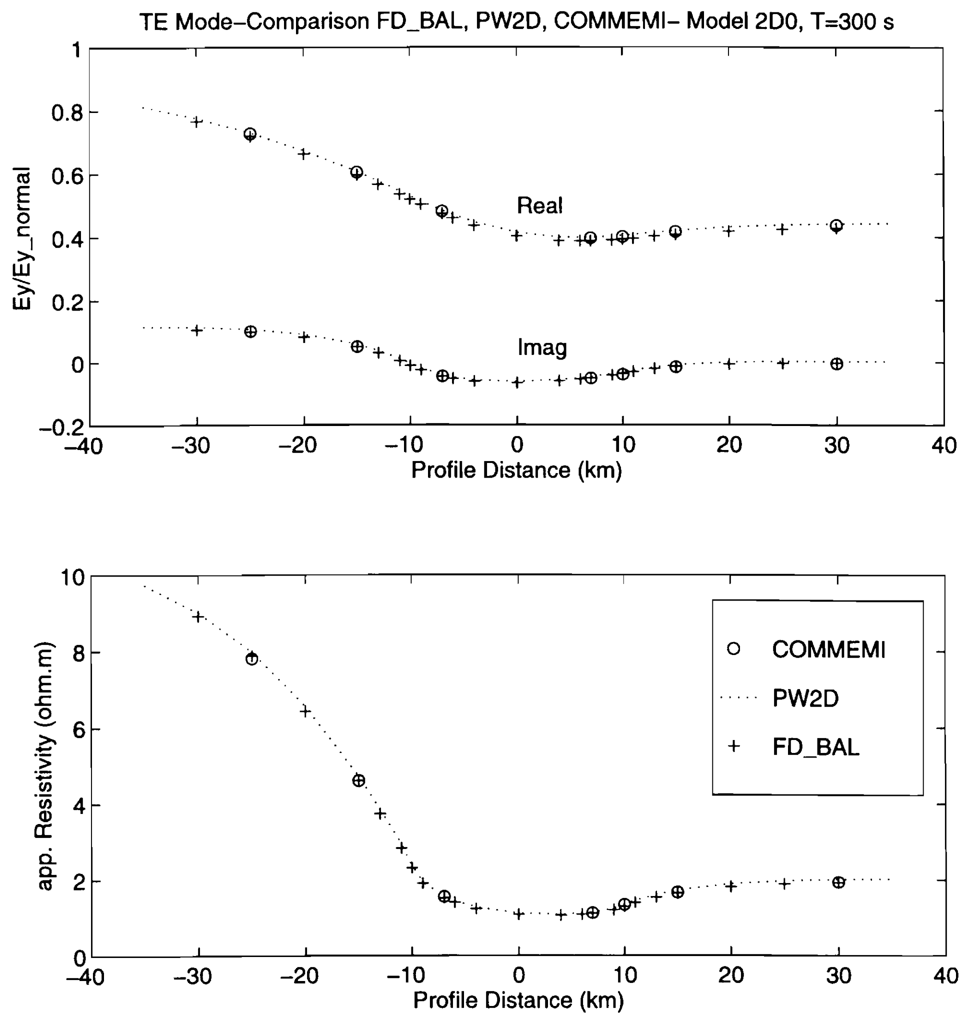

Fig. 2. Comparison of TE mode results from COMMEMI (1990), program PW2D (Wannamaker *et al.*, 1987) and program FD-BAL described here.

of computations. The forward and back substitution used here also consider the banded structure requiring less computations than those for a full matrix. After LU decomposition the system is essentially solved.

The data is usually presented in the form of apparent resistivity ρ^{app} and impedance phase ϕ, both derived from the impedance Z. The expressions for the TE mode are:

$$Z_{TE} = \frac{E_y}{H_x}, \tag{15}$$

$$\rho_{TE}^{app} = \frac{1}{\omega\mu} \left|Z_{TE}\right|^2, \tag{16}$$

$$\phi_{TE} = \arctan \frac{Im Z_{TE}}{Re Z_{TE}}, \tag{17}$$

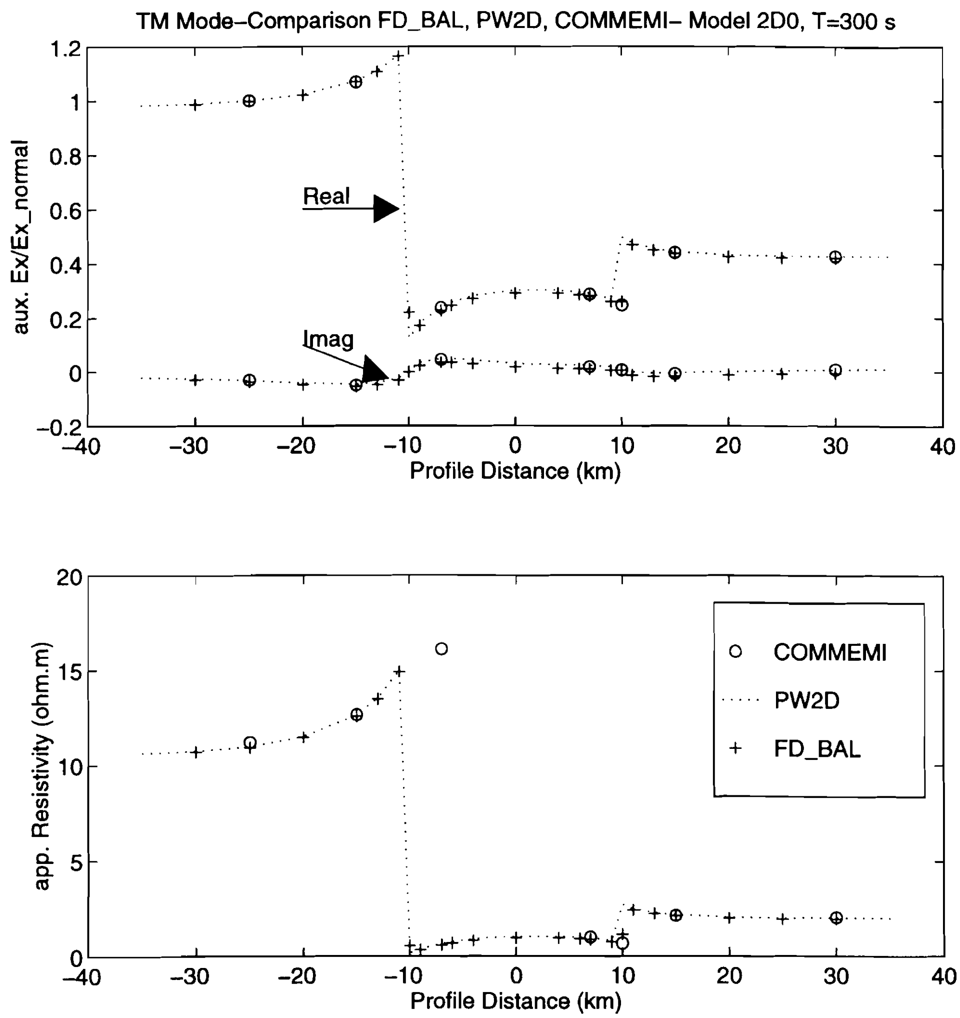

Fig. 3. Comparison of TM mode results from COMMEMI (1990), program PW2D (Wannamaker et al., 1987) and program FD-BAL described here.

and for the TM mode:

$$Z_{TM} = -\frac{E_x}{H_y}, \tag{18}$$

$$\rho_{TM}^{app} = \frac{1}{\omega\mu} |Z_{TM}|^2, \tag{19}$$

$$\phi_{TM} = \arctan \frac{Im Z_{TM}}{Re Z_{TM}}. \tag{20}$$

To validate the solution of our forward code, we present comparisons of results obtained from our finite difference formulation (FD-BAL), from the COMMEMI project (Zhdanov *et al.*, 1990) and from the finite element code of Wannamaker *et al.* (1987), PW2D. The model chosen for demonstration is COMMEMI model 2D-0 (Fig. 1) which consists of three segments of 10, 1 and 2 Ω·m on the top layer underlaid by a perfectly conducting basement. Model 2D-0 has analytical solution (Zhdanov *et al.*, 1990) which enables one to know how well the solution was obtained from a forward code. We also decided to compare our results with those of PW2D since this code is available to us and already checked for the same model in Wannamaker *et al.* (1987). Results for the total electric field parallel to strike E_y, normalized over the total electric field of the normal cross-section E_{ny} at the surface, and for the apparent resistivity for the TE mode are shown in Fig. 2. In Fig. 3, we show results for the total auxiliary electric field perpendicular to strike E_x, normalized over the total electric field of the normal cross-section E_{nx} at the surface, and for the apparent resistivity for the TM mode. Results from FD-BAL agree with both results from COMMEMI and PW2D showing that the forward calculations are valid.

3. Regularized Inverse Solution

The magnetotelluric inverse problem can be formulated using operator notation:

$$Dm = d \tag{21}$$

where D is the forward model operator, m are the model parameters, and d is the set of observed magnetotelluric data.

In the magnetotelluric problem, D is a non-linear operator, the model parameters m are the values of electrical conductivity σ in the earth and d are the values of magnetotelluric impedances (or apparent resistivity and/or phases) recorded on the surface of the earth. However, the magnetotelluric data set is usually contaminated with noise. In inversion, noise in the data can affect the results to produce a formal solution which is far from any realistic model. In other words, small variations in the data set produced by the noise can generate dramatic variations in the inversion solution. For this reason, the magnetotelluric inverse problem is ill-posed.

For the solution of this problem we utilize regularization theory (Tikhonov and Arsenin, 1977) and introduce the parametric functional:

$$P^\alpha(m, d_\delta) = \Theta(m, d) + \alpha S(m) = minimum \tag{22}$$

where $\Theta(m, d) = \|Dm - d\|^2$ is a misfit functional, $S(m) = \|m - m_{apr}\|^2$ is a stabilizing functional and m_{apr} is some *a priori* geoelectrical model.

We use the root mean square of the function m to emphasize the closeness of the solution in terms of some appropriate model m to m_{apr}. This auxiliary condition provides the stability of the solution to the inverse problem.

The *regularization parameter*, α is determined from the misfit condition:

$$\|D(m_\alpha) - d\|^2 = \delta \tag{23}$$

where m_α is the solution to Eq. (22) which minimizes the parametric functional P^α for a given α.

In the practical use of this method for the solution of the inverse magnetotelluric problem, we must remember that along with the continuous function describing the primary data, we have a finite set of these data (measurements of values of the electromagnetic field at a finite number of observation points for specific frequencies). This set of data forms a column vector of length N, which we will designate as $\hat{d}$. In this case, apparent resistivity (ρ^{app}) and impedance phase (ϕ) are usually obtained at several points $(x_1, \ldots, x_n)$ along a profile at several frequencies, ω_1 to ω_m. The vector $\hat{d}$ is:

$$\begin{aligned}\hat{d}^T = [\rho(x_1,\omega_1) \quad \phi(x_1,\omega_1) \quad \rho(x_1,\omega_2) \quad \phi(x_1,\omega_2) \quad \cdots \\ \cdots \quad \rho(x_n,\omega_1) \quad \phi(x_n,\omega_1) \quad \cdots \quad \rho(x_n,\omega_m) \quad \phi(x_n,\omega_m)].\end{aligned}$$

In constructing an initial model for the geoelectric structure of the earth in two dimensions, some organized approach to parameterization must be used in characterizing the spatial distribution of resistivity in the model. In this work this is accomplished by using the same rectangular grid to discretize the earth conductivity model utilized in the forward computations.

After discretizing the field data, d, and distributing conductivities over the model, σ, the solution to the inverse problem stated in Eq. (21) can be written in matrix form:

$$\hat{D}(\hat{m}) = \hat{d} \tag{24}$$

where $\hat{D}$ is the discrete matrix of nonlinear operator D, analogous to the matrix A which appears in the numerical solution of the Maxwell system of equations.

Since the inverse solution to Eq. (21) is ill-posed we search to minimize the misfit parametric functional $P^\alpha(m, d_\delta)$. An additional way to constrain the solution is by introducing weights. The weighting matrix usually contains information on the importance of one data point with relation to the others. In this way, data of better quality will have more importance in the inversion than data of poor quality. If we apply probability theory, the weight matrix is the matrix of data covariances, that is, the weights used are the variance of the data. The parametric functional we seek to minimize is then:

$$P^\alpha(\hat{m}_\alpha, \hat{d}) = \|\hat{W}_d\hat{D}(\hat{m}) - \hat{W}_d\hat{d}\|^2 + \alpha\|\hat{m} - \hat{m}_{apr}\|^2 = minimum, \tag{25}$$

or, if developed:

$$\begin{aligned}P^\alpha(\hat{m}_\alpha, \hat{d}) \quad &= \quad (\hat{W}_d\hat{D}(\hat{m}) - \hat{W}_d\hat{d})^*(\hat{W}_d\hat{D}(\hat{m}) - \hat{W}_d\hat{d}) \\ &\quad + \alpha(\hat{m} - \hat{m}_{apr})^*(\hat{m} - \hat{m}_{apr}) = minimum,\end{aligned} \tag{26}$$

where $\hat{W}_d$ is the weighting diagonal matrix of data, $\hat{m}_{apr}$ is some *a priori* model and "*" means transposed complex conjugated matrix.

The minimization problem (26) gives us the regularized weighted least-squares solution to the inverse problem. The method for solving this problem here, the non-linear conjugate gradient method, is described in the Appendix.

4. Frechet Derivatives

The Frechet derivative matrix is the relationship between the perturbation of the model parameters and the perturbation of the data. Since in magnetotellurics the data is usually presented in the form of apparent resistivity (ρ^{app}) and impedance phase (ϕ), we need to obtain the Frechet terms for these data with respect to the model parameters, the conductivities σ of the model. We obtain a full 2-D Frechet matrix in a quasi-analytical manner utilizing reciprocity (Rodi, 1976; Tripp *et al.*, 1984; Sasaki, 1989) according to the methodology described in de Lugão and Wannamaker (1996). Here we show the derivations to obtain the Frechet terms for the case of our finite difference formulation.

The Frechet terms for apparent resistivity and phase are derived by applying the variational operator δ to Eqs. (16), (17), (19) and (20). For the TE mode, we obtain:

$$\frac{\partial \rho_{TE}^{app}}{\partial \sigma} = \frac{1}{\omega \mu}\left(\frac{\partial Z_{TE}}{\partial \sigma} Z_{TE}^{*} + \frac{\partial Z_{TE}^{*}}{\partial \sigma} Z_{TE}\right) \tag{27}$$

and

$$\frac{\partial \phi_{TE}}{\partial \sigma} = \frac{1}{1+\left(\frac{ImZ_{TE}}{ReZ_{TE}}\right)^2}\left(\frac{\partial ImZ_{TE}}{\partial \sigma} ReZ_{TE} - ImZ_{TE}\frac{\partial ReZ_{TE}}{\partial \sigma}\right)\frac{1}{(ReZ_{TE})^2}. \tag{28}$$

For the TM mode the Frechet terms for apparent resistivity and phase are:

$$\frac{\partial \rho_{TM}^{app}}{\partial \sigma} = \frac{2}{\omega \mu}\left(\frac{\partial Z_{TM}}{\partial \sigma} Z_{TM}^{*} + \frac{\partial Z_{TM}^{*}}{\partial \sigma} Z_{TM}\right) \tag{29}$$

and

$$\frac{\partial \phi_{TM}}{\partial \sigma} = \frac{1}{1+\left(\frac{ImZ_{TM}}{ReZ_{TM}}\right)^2}\left(\frac{\partial ImZ_{TM}}{\partial \sigma} ReZ_{TM} - ImZ_{TM}\frac{\partial ReZ_{TM}}{\partial \sigma}\right)\frac{1}{(ReZ_{TM})^2}. \tag{30}$$

Where the derivative of the impedance with respect to conductivity for the TE mode and resistivity in the TM mode are, respectively:

$$\frac{\partial Z_{TE}}{\partial \sigma} = \frac{1}{H_x^2}\left(\frac{\partial E_y}{\partial \sigma} H_x - \frac{\partial H_x}{\partial \sigma} E_y\right) \tag{31}$$

and

$$\frac{\partial Z_{TM}}{\partial \sigma} = \frac{1}{H_y^2}\left(\frac{\partial E_x}{\partial \sigma} H_y - \frac{\partial H_y}{\partial \sigma} E_x\right). \tag{32}$$

In order to obtain the Frechet derivatives for the magnetotelluric functions above, we need the Frechet for the fields parallel to strike and for the auxiliary fields. We first find the Frechet for the fields parallel to strike F_y by applying the variational operator δ to the finite difference equation (10).

For the TE mode we obtain the following equation:

$$\begin{aligned}\alpha_{ij}^{(0)}\delta E(i,j) &= [\alpha_{ij}^{(1)}\delta E(i+1,j) + \alpha_{ij}^{(2)}\delta E(i,j+1) \\ &\quad + \alpha_{ij}^{(3)}\delta E(i-1,j) + \alpha_{ij}^{(4)}\delta E(i,j-1)] \\ &\quad + E(i,j)\frac{i\omega\mu}{4}\sum_{p=0}^{1}\sum_{q=0}^{1}\delta\sigma_{ij}^{pq}S^{pq}\end{aligned} \tag{33}$$

while for the TM mode the derivation is done in terms of the resistivity ρ, the inverse of the conductivity:

$$\begin{aligned}\alpha_{ij}^{(0)}\delta H(i,j) &= [\alpha_{ij}^{(1)}\delta H(i+1,j) + \alpha_{ij}^{(2)}\delta H(i,j+1) \\ &\quad + \alpha_{ij}^{(3)}\delta H(i-1,j) + \alpha_{ij}^{(4)}\delta H(i,j-1)] \\ &\quad - \delta\alpha_{ij}^{(0)} H(i,j) + [\delta\alpha_{ij}^{(1)} H(i+1,j) + \delta\alpha_{ij}^{(2)} H(i,j+1) \\ &\quad + \delta\alpha_{ij}^{(3)} H(i-1,j) + \delta\alpha_{ij}^{(4)} H(i,j-1)].\end{aligned} \tag{34}$$

The last equations, in matrix notation, can be written almost like Eq. (14) but with a different right hand term.

For the TE mode:

$$\hat{A} \cdot \widehat{\delta E} = \widehat{R}(\delta\sigma) \tag{35}$$

where $\widehat{R}(\delta\sigma)$ is the matrix-column of elements

$$R_{i,j}(\delta\sigma) = E(i,j)\frac{i\omega\mu}{4}\sum_{p=0}^{1}\sum_{q=0}^{1}\delta\sigma_{ij}^{pq}S^{pq}. \tag{36}$$

For the TM mode,

$$\hat{A} \cdot \widehat{\delta H} = \widehat{R}(\delta\rho) \tag{37}$$

where $\widehat{R}(\delta\rho)$ is the matrix-column of elements

$$\begin{aligned} R_{i,j}(\delta\rho) \quad = \quad & \frac{H(i,j)}{-i\omega\mu}\Big[\frac{\sum_{q=0}^{1} S^{1,q}\delta\rho_{ij}^{1,q}}{2(\Delta y_i)^2} + \frac{\sum_{p=0}^{1} S^{p,1}\delta\rho_{ij}^{p,1}}{2(\Delta z_j)^2} \\ & + \frac{\sum_{q=0}^{1} S^{0,q}\delta\rho_{ij}^{0,q}}{2(\Delta y_{i-1})^2} + \frac{\sum_{p=0}^{1} S^{p,0}\delta\rho_{ij}^{p,0}}{2(\Delta z_{z-1})^2}\Big] \\ & + \frac{1}{i\omega\mu}\Big[H(i+1,j)\frac{\sum_{q=0}^{1} S^{1,q}\delta\rho_{ij}^{1,q}}{2(\Delta y_i)^2} + H(i,j+1)\frac{\sum_{p=0}^{1} S^{p,1}\delta\rho_{ij}^{p,1}}{2(\Delta z_j)^2} \\ & + H(i-1,j)\frac{\sum_{q=0}^{1} S^{0,q}\delta\rho_{ij}^{0,q}}{2(\Delta y_{i-1})^2} + H(i,j-1)\frac{\sum_{p=0}^{1} S^{p,0}\delta\rho_{ij}^{p,0}}{2(\Delta z_{z-1})^2}\Big]. \end{aligned} \tag{38}$$

Using the Crout method we have already found the direct triangular decomposition of the matrix $\hat{A}$ and solving the two simple forward and back substitution systems we can determine the variation in the fields $\widehat{\delta E}$ and $\widehat{\delta H}$ for any perturbation in the conductivity $\delta\sigma_{ij}^{pq}$ or resistivity $\delta\rho_{ij}^{pq}$ of the model.

From the general theory of variational calculus:

$$\delta Ax = A(x+\delta x) - A(x) \approx Fre_x(\delta x) = \delta A(x, \delta x). \tag{39}$$

In our case

$$\widehat{\delta E} = \widehat{Fre_\sigma}\widehat{\delta\sigma} \tag{40}$$

and

$$\widehat{\delta H} = \widehat{Fre_\rho}\widehat{\delta\rho} \tag{41}$$

where $\widehat{\delta\sigma}$ and $\widehat{\delta\rho}$ are the matrix-columns of model parameters perturbed. Thus, to determine the columns of the Frechet derivative matrix, we have to substitute on the place of $\widehat{\delta\sigma}$ in Eq. (40) and $\widehat{\delta\rho}$ in Eq. (41) a matrix-column with nonzeros only on the rows corresponding to the fields perturbed by $\delta\sigma_{ij}$ (or $\delta\rho_{ij}$):

$$\begin{bmatrix} R_i(1) \\ 0 \\ \vdots \\ 0 \end{bmatrix}.$$

The procedure described until here is analogous to the one utilized in the Occam code of de Groot-Hedlin and Constable (1990). In that procedure, forward and back substitutions need to be performed for, at least, the number of inversion parameters, which can reach the order of thousands.

Perturbation of each inversion parameter introduces a term in the RHS of Eqs. (35) and (37) that can be seen as a source placed at the nodes adjacent to the cell/parameter. However, according to reciprocity (Rodi, 1976), the role of a unit source placed at a node inside the mesh, can be interchanged with that of a unit source placed at the receiver of interest.

$$\hat{A} \cdot \hat{G} = \hat{U}(1). \tag{42}$$

Solving the systems with these unit sources yields vector $\hat{G}$ containing the responses at all nodes in the mesh.

To obtain the Frechet terms at the nodes which correspond to the perturbation of each cell/parameter we only need to multiply vector $\widehat{G}$ by the cell parameters. In the TE mode, this

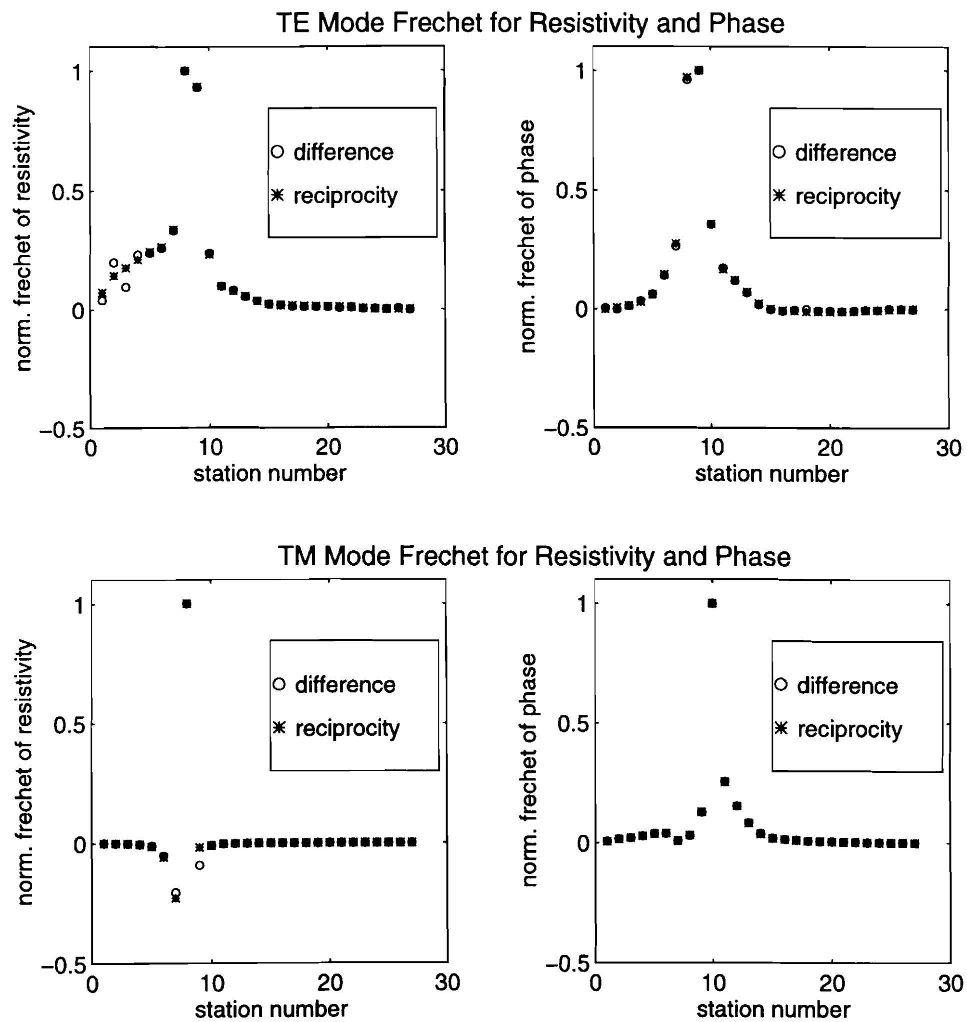

Fig. 4. Comparison of calculation of Frechet terms obtained from difference of perturbed and unperturbed forward solutions and analytical calculation utilizing reciprocity for apparent resistivity and phase for the TE and TM modes.

procedure is:

$$\widehat{\delta E} = \hat{G}\left(E(i,j)\frac{i\omega\mu}{4}\sum_{p=0}^{1}\sum_{q=0}^{1} S^{pq}\right). \tag{43}$$

In the TM mode, the cell parameters multiplied by the solution to the unit source is:

$$\begin{aligned}\widehat{\delta H} \quad = \quad & \hat{G}\frac{H(i,j)}{-i\omega\mu}\left[\frac{\sum_{q=0}^{1} S^{1,q}}{2(\Delta y_i)^2} + \frac{\sum_{p=0}^{1} S^{p,1}}{2(\Delta z_j)^2} + \frac{\sum_{q=0}^{1} S^{0,q}}{2(\Delta y_{i-1})^2} + \frac{\sum_{p=0}^{1} S^{p,0}}{2(\Delta z_{z-1})^2}\right] \\ & + \frac{1}{i\omega\mu}\left[H(i+1,j)\frac{\sum_{q=0}^{1} S^{1,q}}{2(\Delta y_i)^2} + H(i,j+1)\frac{\sum_{p=0}^{1} S^{p,1}}{2(\Delta z_j)^2}\right. \\ & \left. + H(i-1,j)\frac{\sum_{q=0}^{1} S^{0,q}}{2(\Delta y_{i-1})^2} + H(i,j-1)\frac{\sum_{p=0}^{1} S^{p,0}}{2(\Delta z_{z-1})^2}\right].\end{aligned} \tag{44}$$

After the Frechet terms are obtained for the fields parallel to strike, we need to obtain the auxiliary field Frechets. The calculation of the Frechet terms for the auxiliary fields also follows that of de Lugão and Wannamaker (1996). Equations (2) and (3) (TE mode), and Eqs. (5) and (6) (TM mode) are differentiated with respect to the model parameters $\widehat{\delta\sigma}$ or $\widehat{\delta\rho}$. The Frechet terms for the parallel fields are then used in the finite difference approximation to these equations.

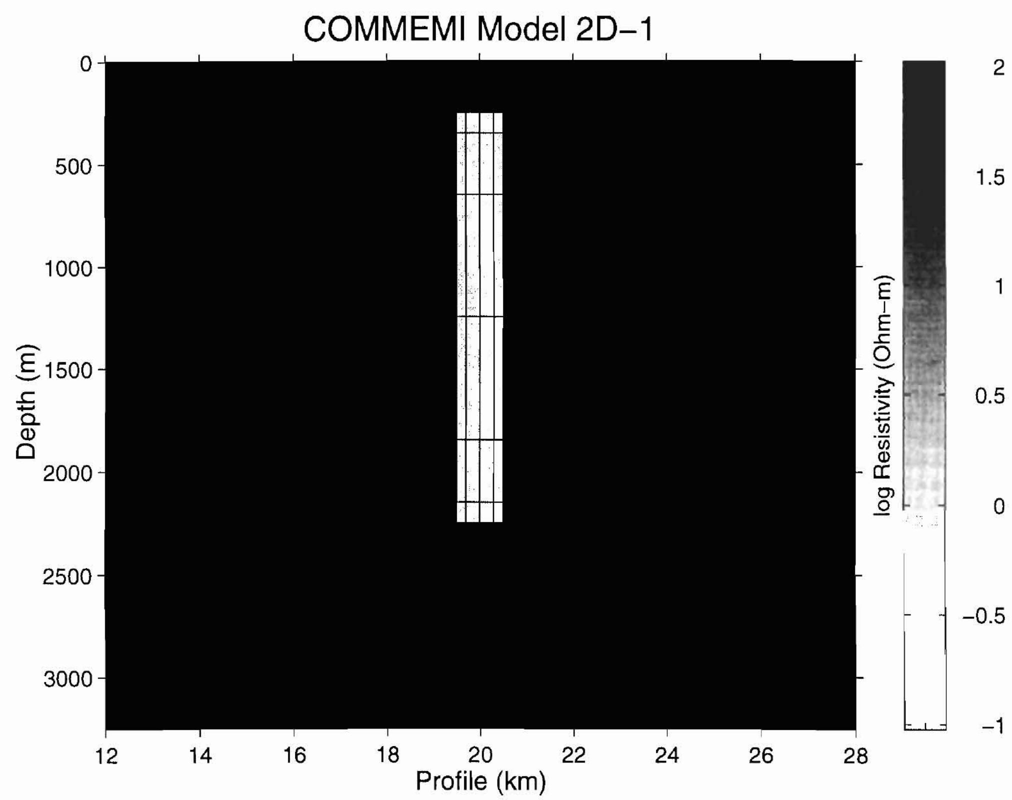

Fig. 5. COMMEMI model 2D-1 used to generate synthetic apparent resistivity and phase data.

For the TE mode, the Frechet components of the auxiliary magnetic field are:

$$\frac{\partial H_x}{\partial \sigma} = -\frac{1}{i\omega\mu_0}\frac{\partial}{\partial z}\frac{\partial E_y}{\partial \sigma} \tag{45}$$

and,

$$\frac{\partial H_z}{\partial \sigma} = \frac{1}{i\omega\mu_0}\frac{\partial}{\partial x}\frac{\partial E_y}{\partial \sigma}. \tag{46}$$

For the TM mode, the Frechet components of the auxiliary electric field are:

$$\frac{\partial E_x}{\partial \rho} = \frac{1}{\rho}E_x - \rho\frac{\partial}{\partial z}\frac{\partial H_y}{\partial \rho} \tag{47}$$

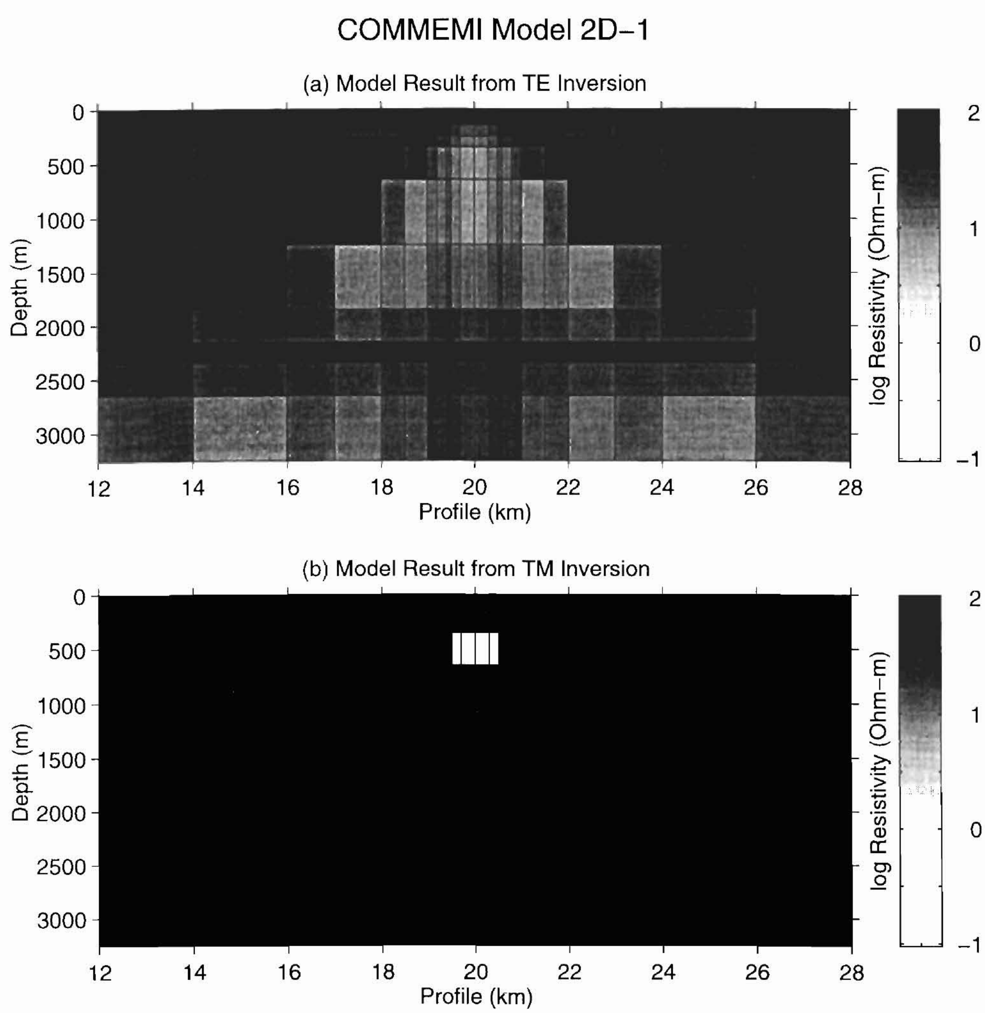

Fig. 6. Resistivity models resulting from inversion of TE (a) and TM (b) mode synthetic data from COMMEMI model 2D-1.

and,

$$\frac{\partial E_z}{\partial \rho} = \frac{1}{\rho} E_z + \rho \frac{\partial}{\partial x} \frac{\partial H_y}{\partial \rho}. \tag{48}$$

Instead of a unit placed at the receiver on the RHS vector of Eqs. (35) and (37), weighted values corresponding to the finite difference coefficients used in the approximations of Eqs. (45), (46), (47) and (48) are loaded in the locations of the fields used in the finite difference approximation. The result is again a vector $\hat{G}$ of responses that correspond to a perturbation at the receiver of interest due to perturbation at all nodes in the mesh. This response $\hat{G}$ is then multiplied by the cell parameters of interest as in Eqs. (43) and (44). By utilizing reciprocity, the number of forward and back substitutions that need to be performed in order to obtain the Frechet terms is now in the order of receivers of interest, which are usually less than one hundred in an MT survey.

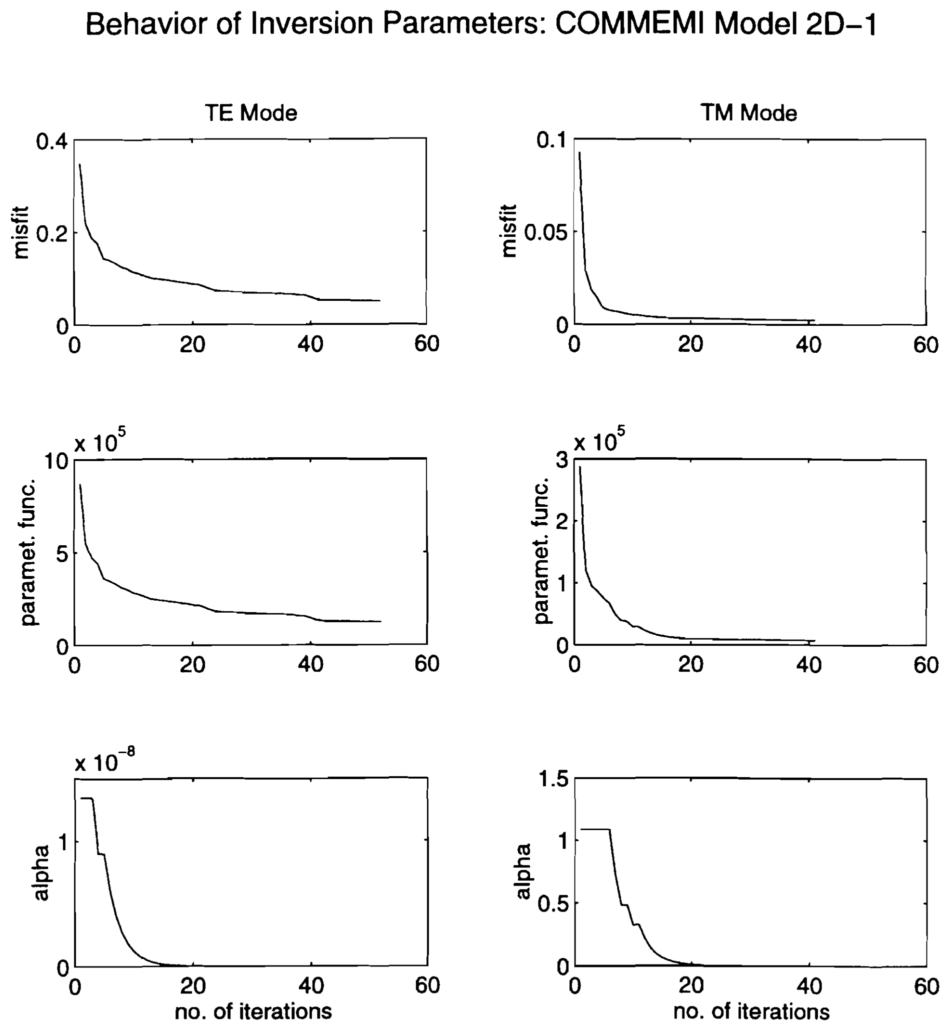

Fig. 7. Behavior of normalized misfit, parametric functional and regularization parameter (α) for TE and TM mode inversion of COMMEMI model 2D-1.

Figure 4 shows comparison of calculation of Frechet terms for apparent resistivity and phase for both TE and TM modes for all nodes (corresponding to stations) at the surface. The perturbed parameter was the resistivity on the cell on the first row and ninth column of COMMEMI model 2D-0 (Fig. 1) and the period used was 300 s. We compare results calculated using reciprocity with the results obtained by the difference between two forward solutions (unperturbed and perturbing the resistivity value by 10%). The results are normalized by their maximum values, so that the unit value corresponds to the maximum perturbation. The agreement between values obtained with reciprocity and by difference of two forward solutions is within machine precision, with some small discrepancies which do not affect the inversion results.

5. Inversion of Synthetic Data

In order to test the inversion algorithm, we performed inversion for sets of synthetic data with no noise added to them. The stoping criteria chosen were either to reach a maximum number

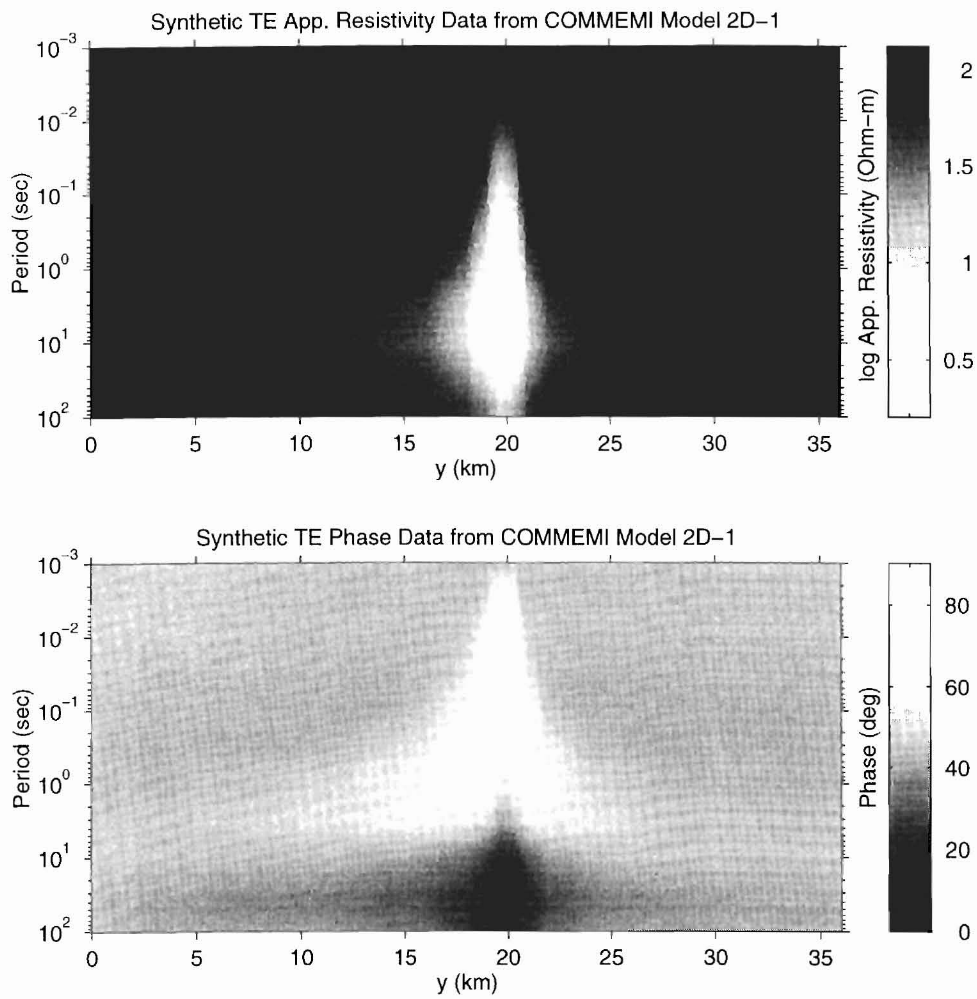

Fig. 8. Pseudosections of TE mode synthetic data from COMMEMI model 2D-1.

of iterations or a minimum misfit, which was calculated as the ratio:

$$\frac{\|\hat{D}\hat{m} - \hat{d}\|^2}{\|\hat{d}\|^2}.$$

Also, in order to constrain the values of inversion parameters (resistivities) to be positive, maximum and minimum values that these resistivity can have are input as additional inversion parameters. In this particular case these were, respectively, 1000. and 0.1 Ω·m. The starting model used in the inversion is the *a priori* model used in the regularization.

Two sets of synthetic apparent resistivity and phase data for TE and TM modes were generated using COMMEMI model 2D-1, shown in Fig. 5. COMMEMI model 2D-1 consists of a 0.5 Ω·m conductor buried in a 100 Ω·m background. Eleven frequencies (0.01, 0.03, 0.1, 0.3, 1., 3., 10., 30., 100., 300. and 1000. Hz) were used to generate data for 27 stations located at the surface. The mesh used in the forward calculations consisted of 12 rows of 28 rectangles each in

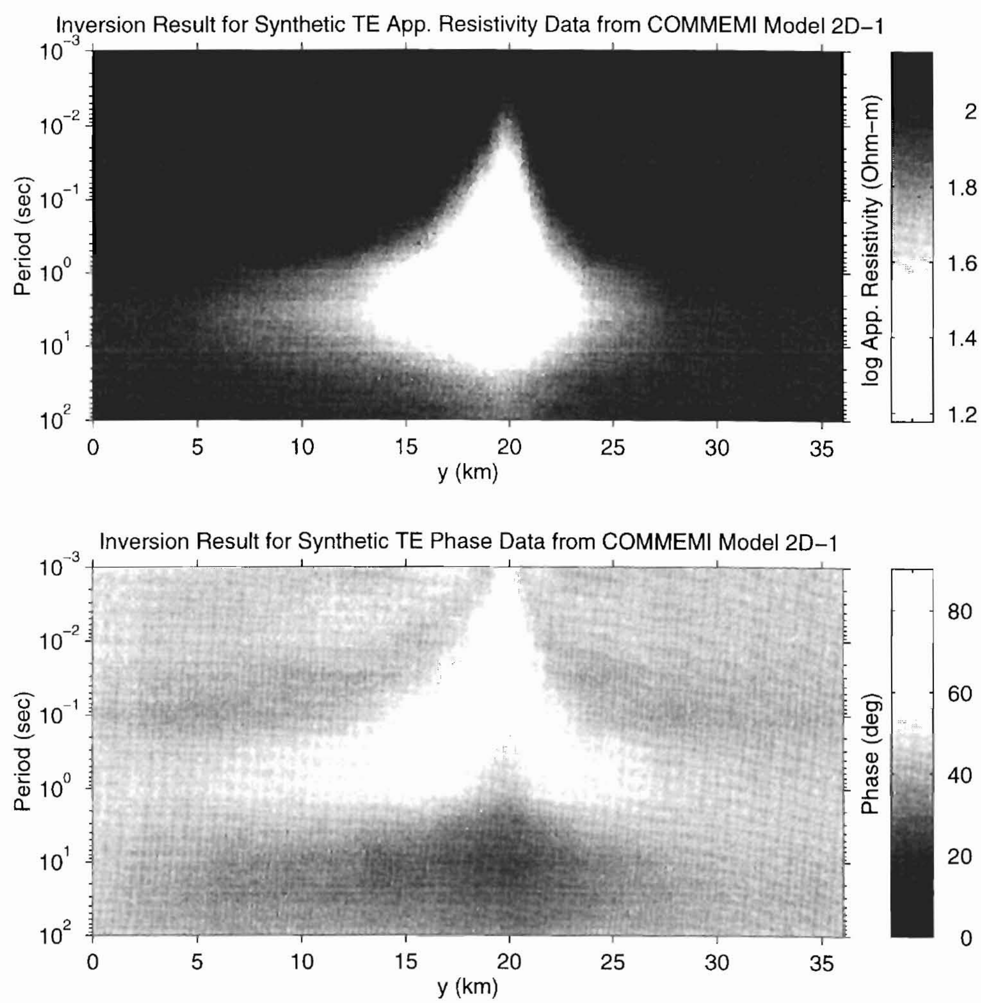

Fig. 9. Pseudosections of data resulting from inversion of synthetic TE mode data from COMMEMI model 2D-1.

a total of 336 rectangular cells. This same mesh was used in the inversion.

We performed inversion for TE and TM modes separately. Starting models were a 100 Ω·m half-space and inversion parameters were all 336 resistivities in the rectangular cells for both TE and TM mode inversions. All calculations were performed on a Pentium 100 MHz.

Inversion for TE mode apparent resistivity and phase data for a misfit of 0.05 yielded the model shown in Fig. 6(a). The misfit was achieved after 52 iterations; each iteration taking 17 minutes. The inversion of TM mode data, however, took only 6 minutes per iteration since this mode does not require air layers on top of the mesh, resulting in a smaller matrix system. A 0.002 misfit was reached after 41 iterations and resulted in the model shown in Fig. 6(b).

Figure 7 shows the behavior of normalized misfit, parametric functional and how the regularization parameter α was changed throughout both TE and TM inversion processes. A stable minimization was observed for both, normalized misfit and parametric functional, at each iteration until the desired misfits were obtained.

Neither TE nor TM modes alone could recover the original model of Fig. 5 due to the

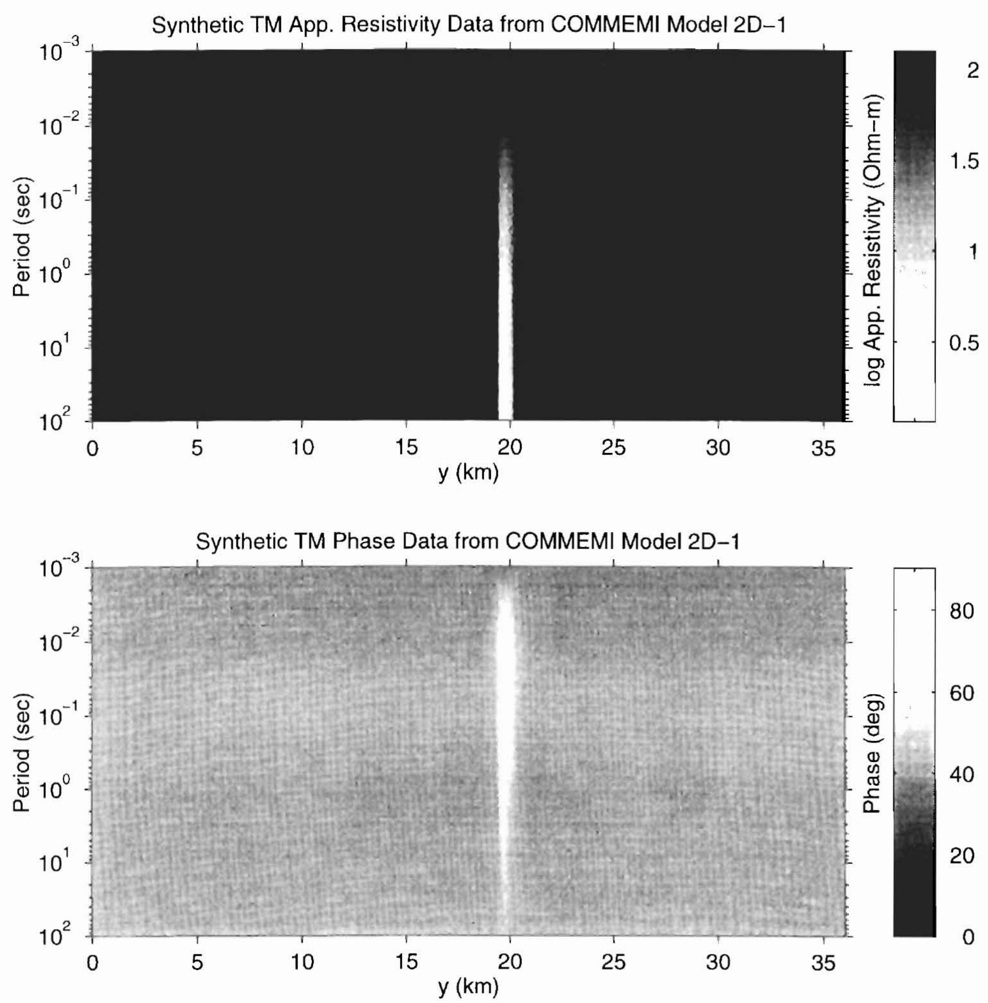

Fig. 10. Pseudosections of TM mode synthetic data from COMMEMI model 2D-1.

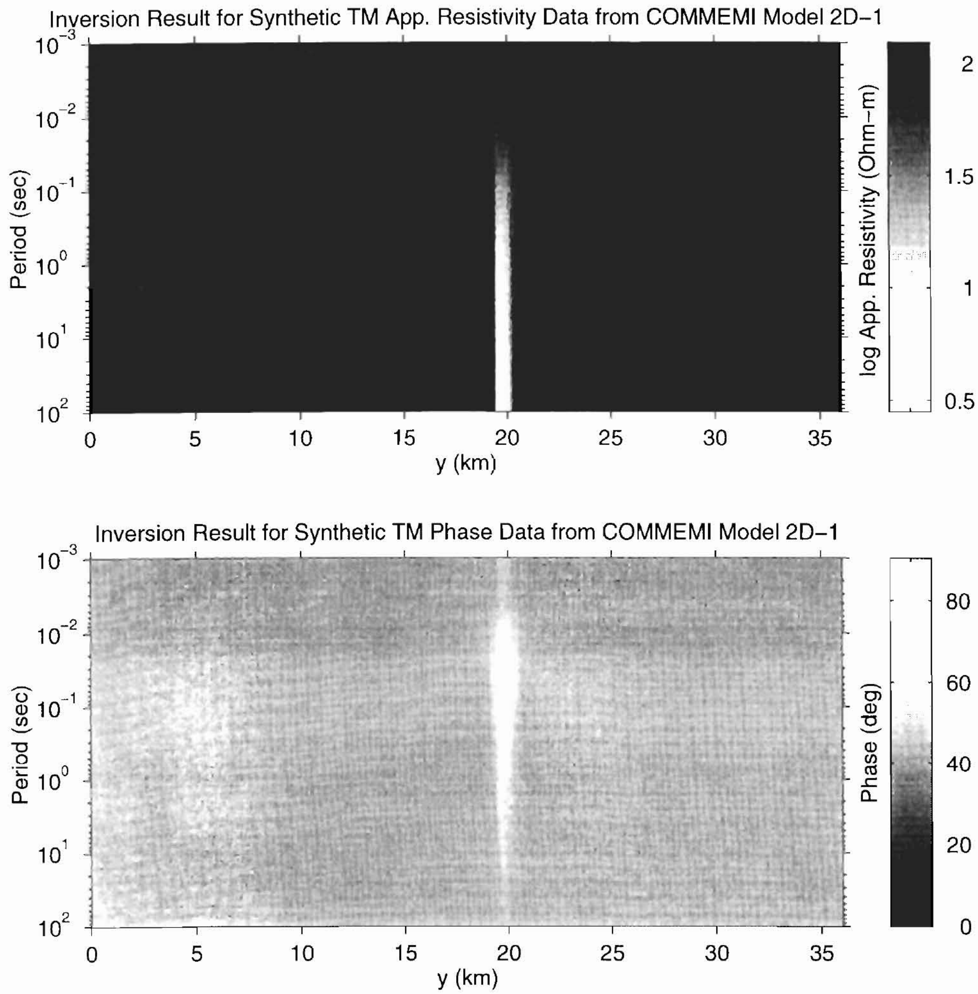

Fig. 11. Pseudosections of data resulting from inversion of synthetic TM mode data from COMMEMI model 2D-1.

inherent non-uniqueness of the inverse problem. However, these models are consistent with the resolution of each mode separately. The model obatined from TM inversion (Fig. 6(b)) recovers a smaller and more conductive body at the right location, while the result from the TE inversion (Fig. 6(a)) shows a resistive top with a large conductive body that extends to depth. Also, both models generate sets of apparent resistivity and phase data that agree to the original synthetic within the specified misfit. Figures 8 and 9 show pseudosections for original data and the one obtained from inversion, respectively, for the TE mode, while Figs. 10 and 11 show the same result for the TM mode. We generated these pseudosections in order to compare the original synthetic data to that obtained from the inversions. These pseudosections show that the result from inversion of synthetic data yields acceptable results.

6. Inversion of CSAMT Data from Kennecott Exploration

A set of controlled source audio-frequency magnetotelluric (CSAMT) field data from Kennecott Exploration, with drill control available for comparison, is interpreted using the two-dimensional inversion scheme described here. CSAMT is a resistivity mapping tool which has excellent lateral resolution, depth penetration and field production. A controlled source is used to overcome problems with unstable natural source fields that are encountered in audio-frequency magnetotelluric (AMT) surveys. CSAMT data interpretation was typically achieved by one-dimensional pseudo-depth plots or inversions, which are distorted by static shift and terrain effects. Two-dimensional inversion and interpretation of plane-wave CSAMT data should help remove these artifacts and produce a geologically reasonable resistivity model. Source effects, which typically contaminate low-frequency CSAMT data, are difficult to interpret and are discarded in this scheme.

A total of 15 CSAMT stations, spaced 100 meters apart and for eleven frequencies (8192., 4096., 2048., 1024., 512., 256., 128., 64., 32., 16. and 8. Hz) were collected over a profile where Kennecott has located quartz-porphyry dikes, breccia and sulfide veins cutting Cretaceous sandstone and limestone host rocks. Resistivity variations in the observed data are caused by faulting, by high-resistivity quartz-porphyry dikes and by low-resistivity sulfide veins.

A geological cross-section for the area along the profile where the data were acquired is shown in Fig. 12. Results from smooth 1-D inversions of each 15 stations, provided by Kennecott, are plotted as a combined section in Fig. 13. The combined 1-D section resolves the location of the quartz porphyry and another resistive feature close to station −150, which may be associated to

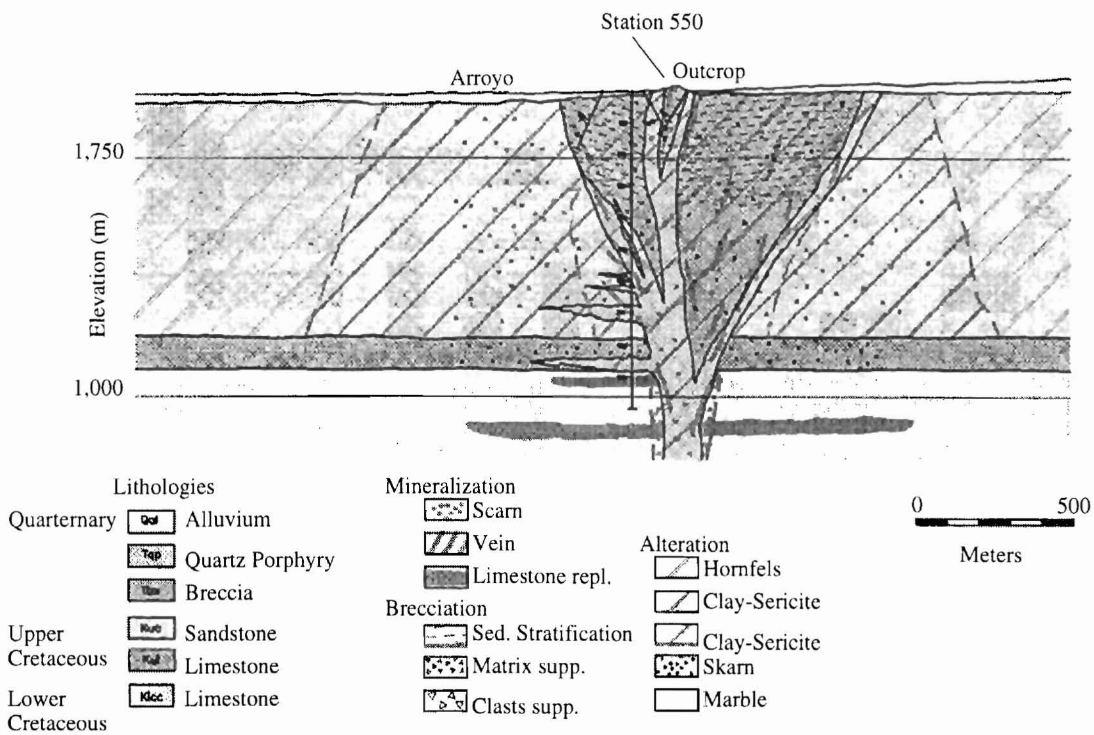

Fig. 12. Geological cross-section along profile of CSAMT data from Kennecott Exploration.

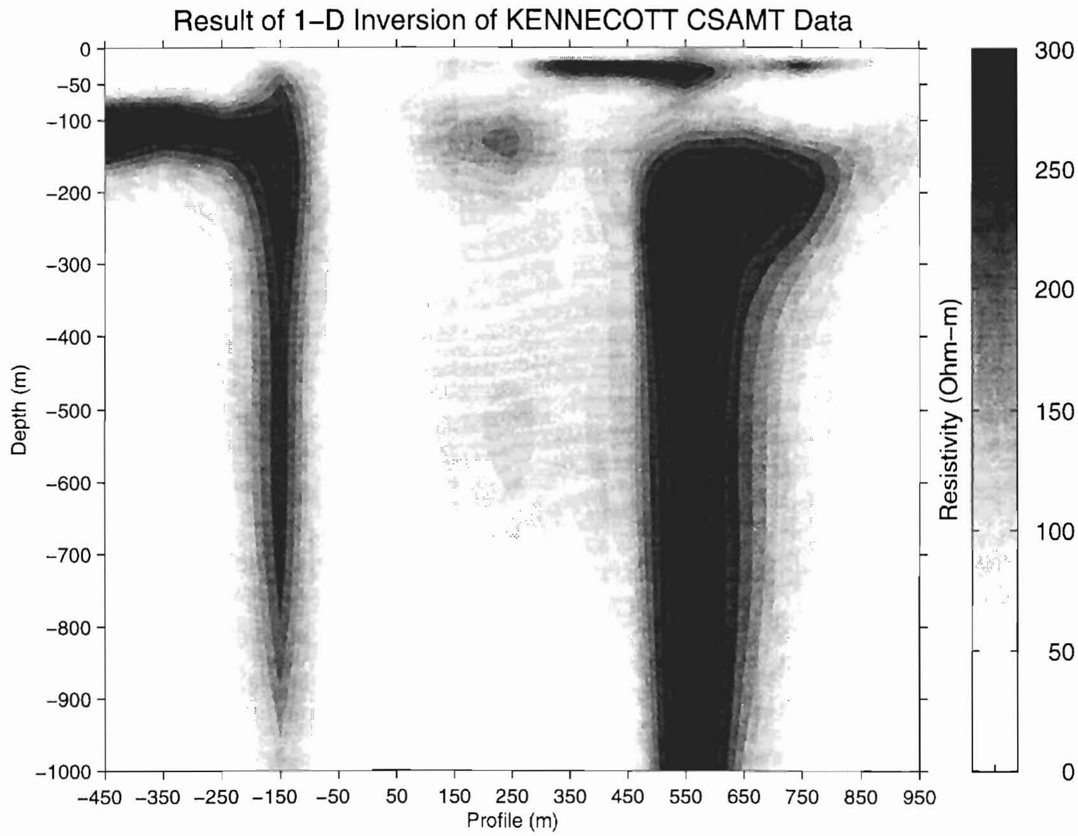

Fig. 13. Combined section of independent results from 1-D inversions of each station of CSAMT data from Kennecott Exploration.

a fault. However, both resistive features are very elongated, a behavior typical of 1-D results.

Laboratory studies of the physical properties of the rocks found in the area yielded resistivity values between 13 and 2723 Ω·m for the sandstones, between 38 and 2462 Ω·m for breccia, and between 9900 and 37000 Ω·m for the quartz porphyry. The lowest resistivity values for the sandstones and for the breccia are associated to the presence of lead-silver zinc veins.

All the geological, laboratory and 1-D inversion information provided was used to construct the 2-D starting model shown in Fig. 14(a). Also, maximum and minimum resistivity values in the model were constrained between 13 and 37000 Ω·m, based on the laboratory values.

Two-dimensional inversion was performed for data in the plane-wave regime (10 frequencies: 8192 to 16 Hz) for all 15 stations. The mesh constructed had 11 rows and 16 columns, in a total of 176 rectangular cells. The inversion parameters were all 176 resistivities of these cells and the calculations were performed on a Pentium 100 MHz. Total inversion time was 17 minutes for 13 iterations to reach a misfit of 0.02 and converge to the model shown in Fig. 14(b). Apparent resistivity and phase pseudosections of the observed data are shown in Fig. 15. These can be compared to pseudosections of the data obtained from inversion (Fig. 16) which depict all the major features seen in the observed data.

The behavior of misfit and parametric functional (Fig. 17) was stable throughout the inversion process. Figure 17 also shows the behavior of the regularization parameter α and how the value

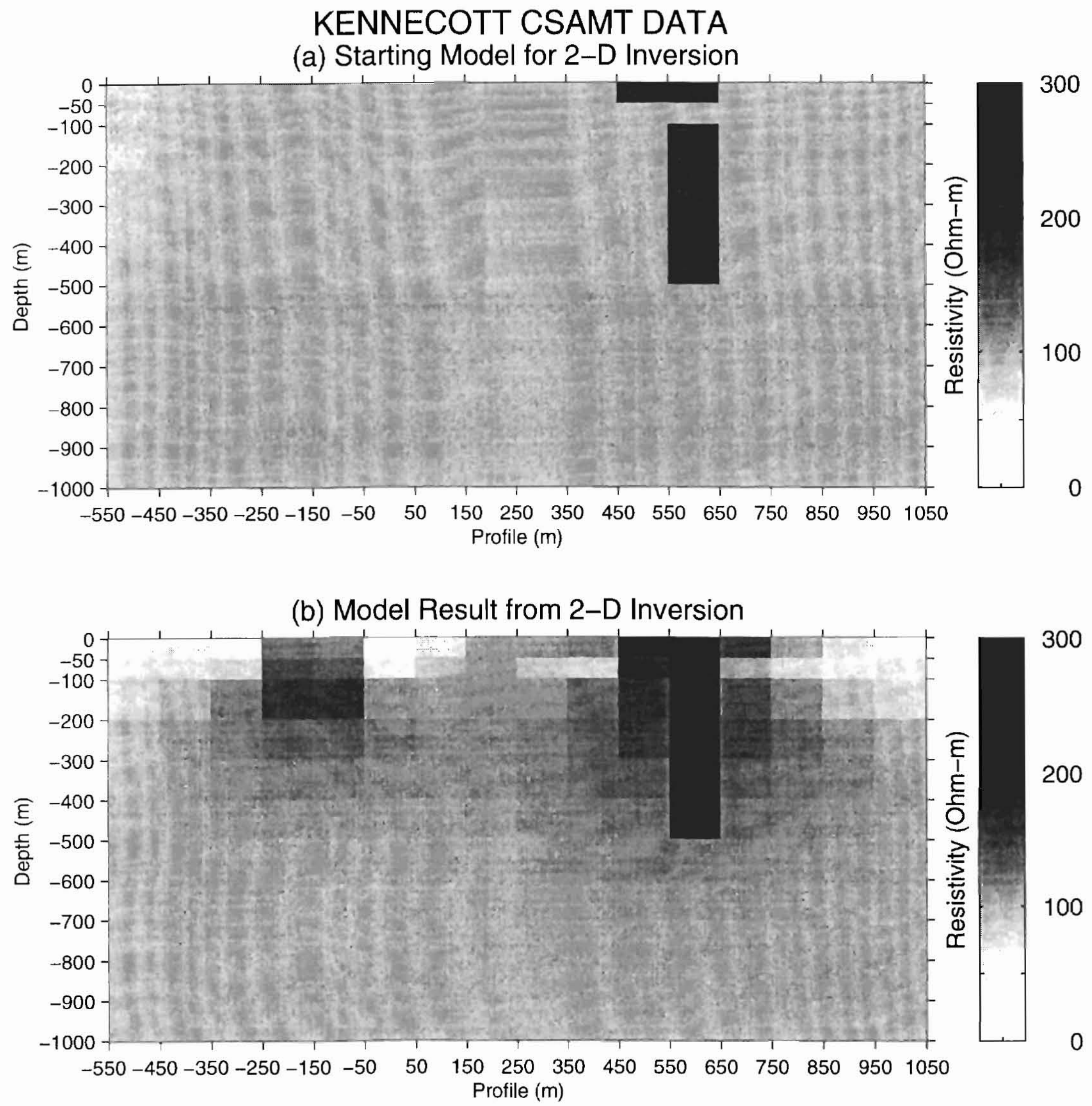

Fig. 14. Starting model (a) and resistivity model (b) result from TM mode 2-D inversion of CSAMT data from Kennecott Exploration.

was changed during the inversion.

The model obtained from 2-D inversion (Fig. 14(b)) reinforces the location of the quartz porphyry by increasing the resistivity of the body below station 550. Other features, such as the resistor below station −150, also appear in the 2-D model, but without the elongated pattern. However, in order to test if the resistive body at station 550 was required by the data or was just an artifact from its presence in the starting model, inversion was performed for the same data and with the same parameters but with a 100 Ω·m half-space as starting model. The resulting model is shown in Fig. 18 and it does show the same resistive structures at station 550 and −150, consistent with the location of the quartz porphyry and a possible fault. The behavior

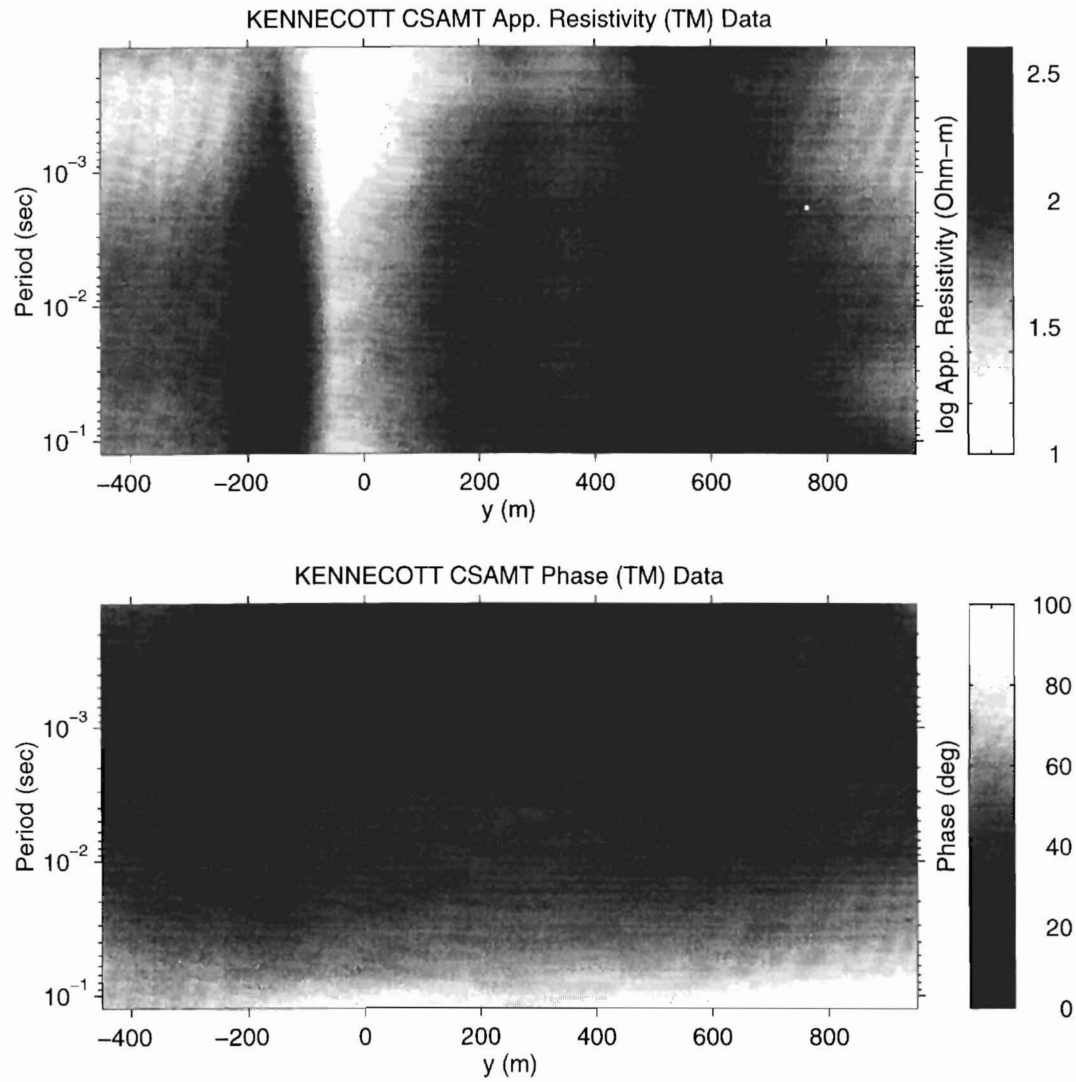

Fig. 15. Pseudosections of apparent resistivity and phase CSAMT data (TM mode) from Kennecott Exploration.

of inversion parameters is shown in Fig. 19 and it took 15 iterations to reach the 0.02 misfit, 2 more iterations than when some *a priori* information was utilized in the starting model. The plane-wave apparent resistivity and phase data obtained for this inversion are shown in Fig. 20 and they, too, depict most features of the original data (Fig. 15). These results show that the model obtained from inversion is affected little by the starting model, provided that the initial guess is based on accurate geological information.

We should also notice that these highly resistive structures are very difficult to resolve by CSAMT data. It is very well known that inductive techniques have low sensitivity to resistive targets. That is why we can consider these results from 2-D inversion, with respect to the quartz porphyry body and possible location of fault structure at station −150, as a success. The two-dimensional inversion of plane-wave CSAMT data has accurately resolved known quartz porphyry

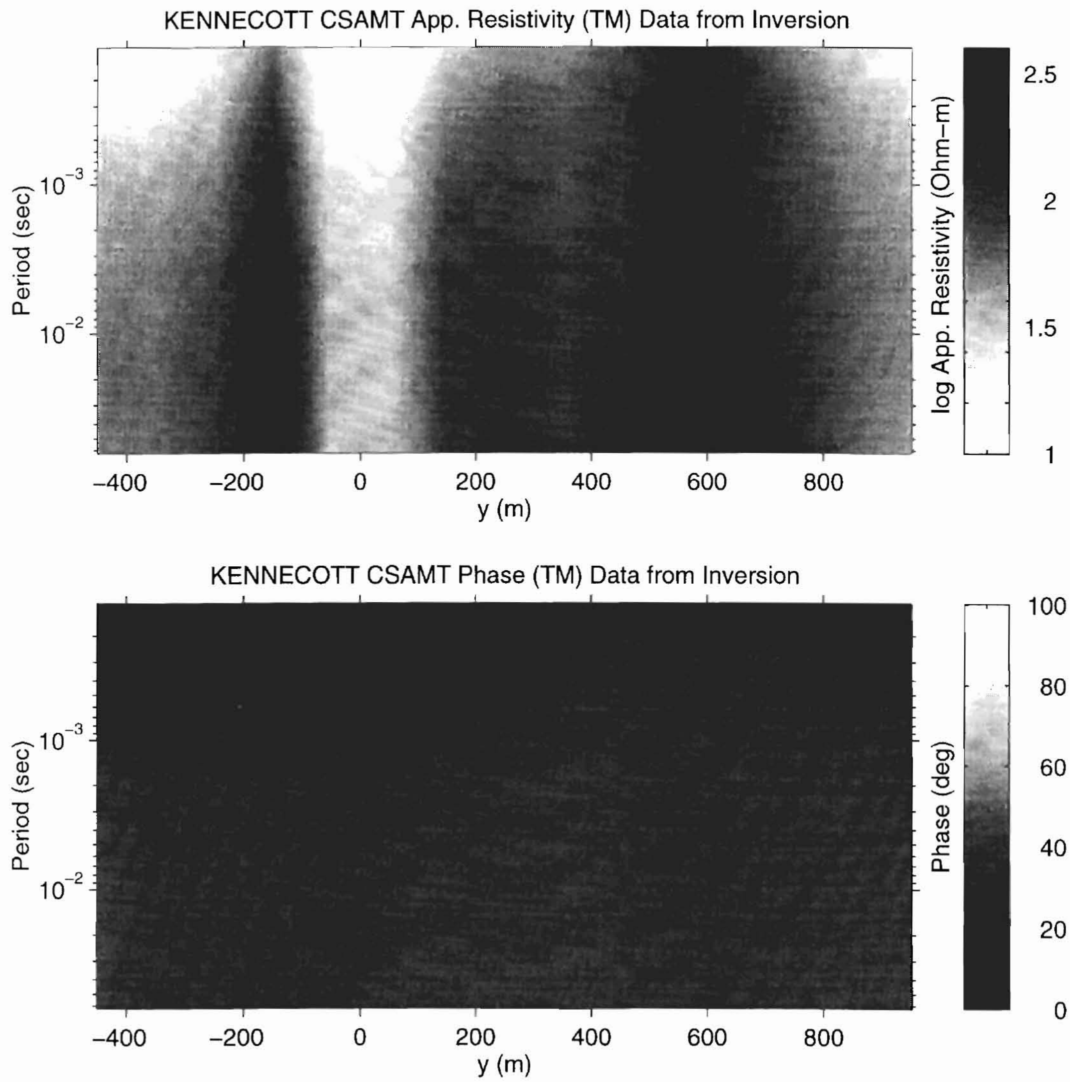

Fig. 16. Pseudosections of apparent resistivity and phase CSAMT data resulting from TM mode 2-D inversion of Kennecott Exploration data.

dikes as well as new structural targets.

7. Conclusions

This work presents an approach for the solution of overparameterized 2-D MT inversion problems that deals with the model of an arbitrary structure.

For the forward solution, we use a fast and efficient finite difference formulation to the solution of both TE and TM modes in MT based on a modification of the balance method. The forward code was then checked against known solutions and existing codes.

A full 2-D Frechet derivative matrix is obtained as a solution to simple forward and back substitution of the LU decomposed matrix of coefficients from the forward problem with a different

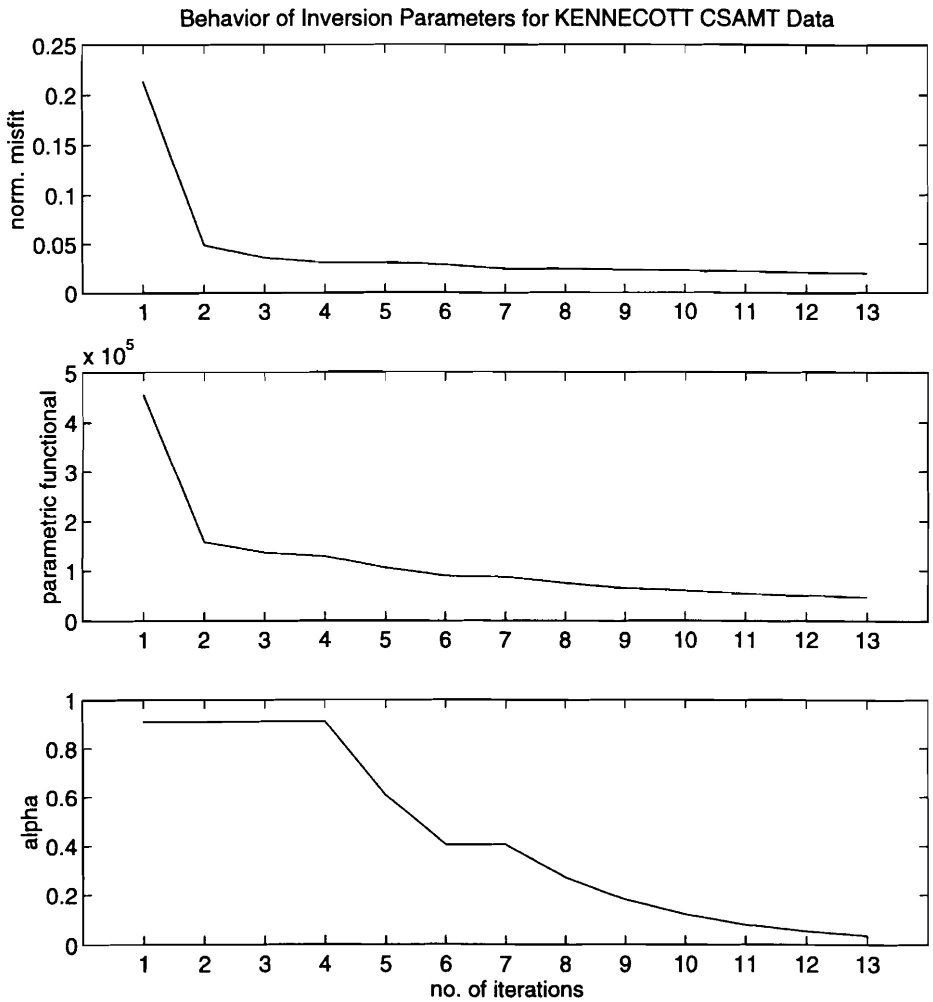

Fig. 17. Behavior of normalized misfit, parametric functional and regularization parameter (α) for TM mode inversion of Kennecott Exploration CSAMT data.

right hand term and utilizing the principle of reciprocity.

In order to constrain the solutions of the inverse problem to a set of possible models, a stabilizing functional was introduced, referencing the solution to an *a priori* model.

The inverse code was first tested and provided fast and stable results for synthetic data sets within the resolution of each mode separately. Also, results of practical application of the method to CSAMT data from Kennecott Exploration demonstrate its effectiveness in the inversion of real data sets by resolving known and possible new structural targets.

By utilizing an accurate and simple finite-difference formulation, reciprocity in calculation of the Frechet matrix, and by regularizing the inverse problem by referencing to an *a priori* model we constructed a method which is fast, stable and that provides geologically reasonable results which can help in the interpretation of MT and plane-wave CSAMT data.

The authors thank the Consortium for Electromagnetic Modeling and Inversion (CEMI) at the

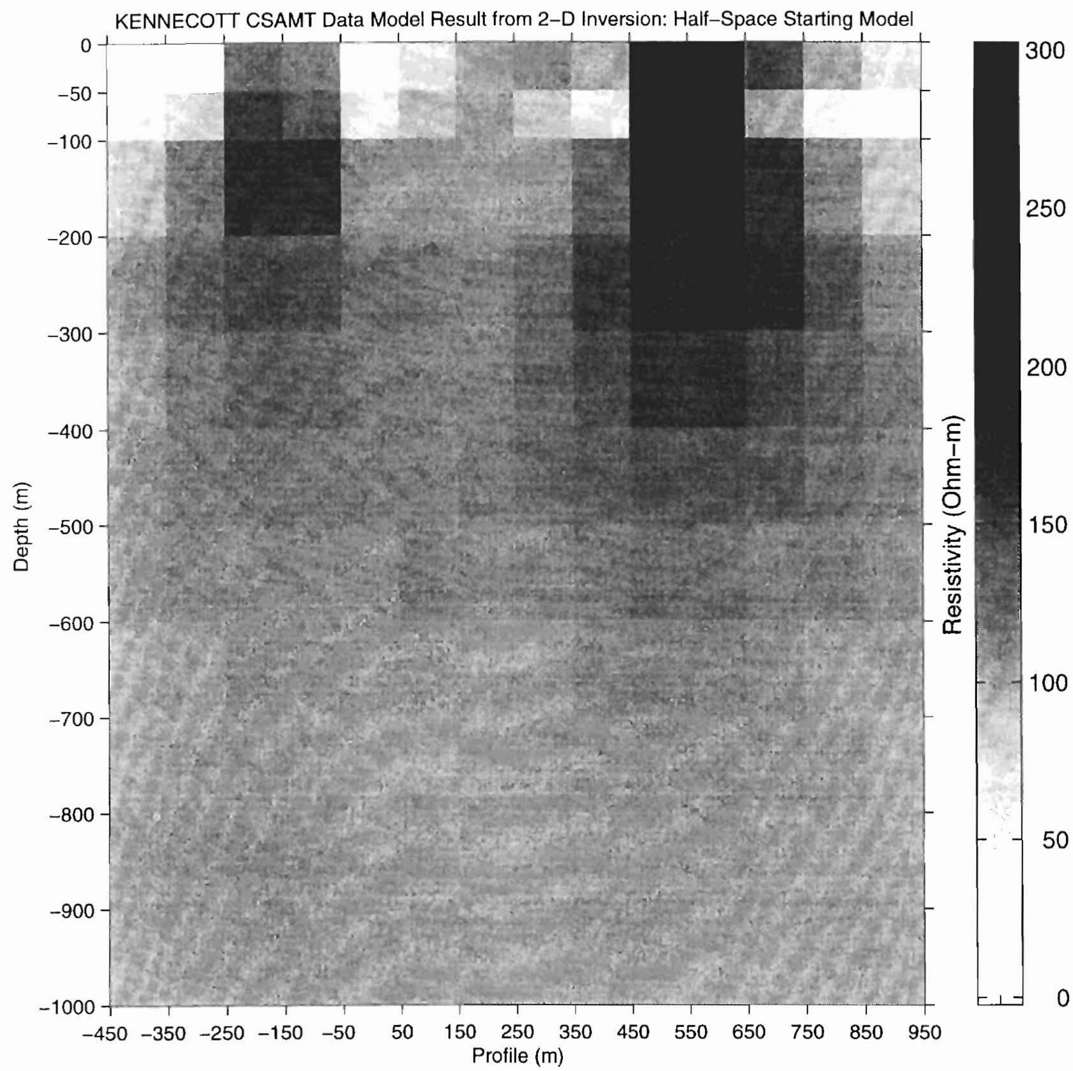

Fig. 18. Resistivity model resulting from TM mode 2-D inversion of CSAMT data from Kennecott Exploration utilizing a 100 Ω·m half-space as starting model.

Department of Geology and Geophysics, University of Utah, including CRA Exploration, Newmont Exploration, Western Mining, Kennecott Exploration, Schlumberger-Doll Research, Shell Exploratie en Produktie Laboratorium, Western Atlas, United States Geological Survey, Zonge Engineering, Mindeco, MIM Exploration, BHP Minerals, Naval Research Laboratory and Unocal Geothermal for support of this work. One of the authors, Patricia Pastana de Lugão, is being supported by a scholarship provided by the Brazilian government through CNPq (Conselho Nacional de Pesquisa). The authors wish to thank Hans Rasmussen from Kennecott Exploration for providing the CSAMT data and geological information in the area and Berthold Kriegshäuser for providing many usefull comments and help with the figures. The authors also wish to thank the reviewers, Dr. Ashok Agarwal and Dr. Yuji Mitsuhata, for improving the manuscript with their suggestions.

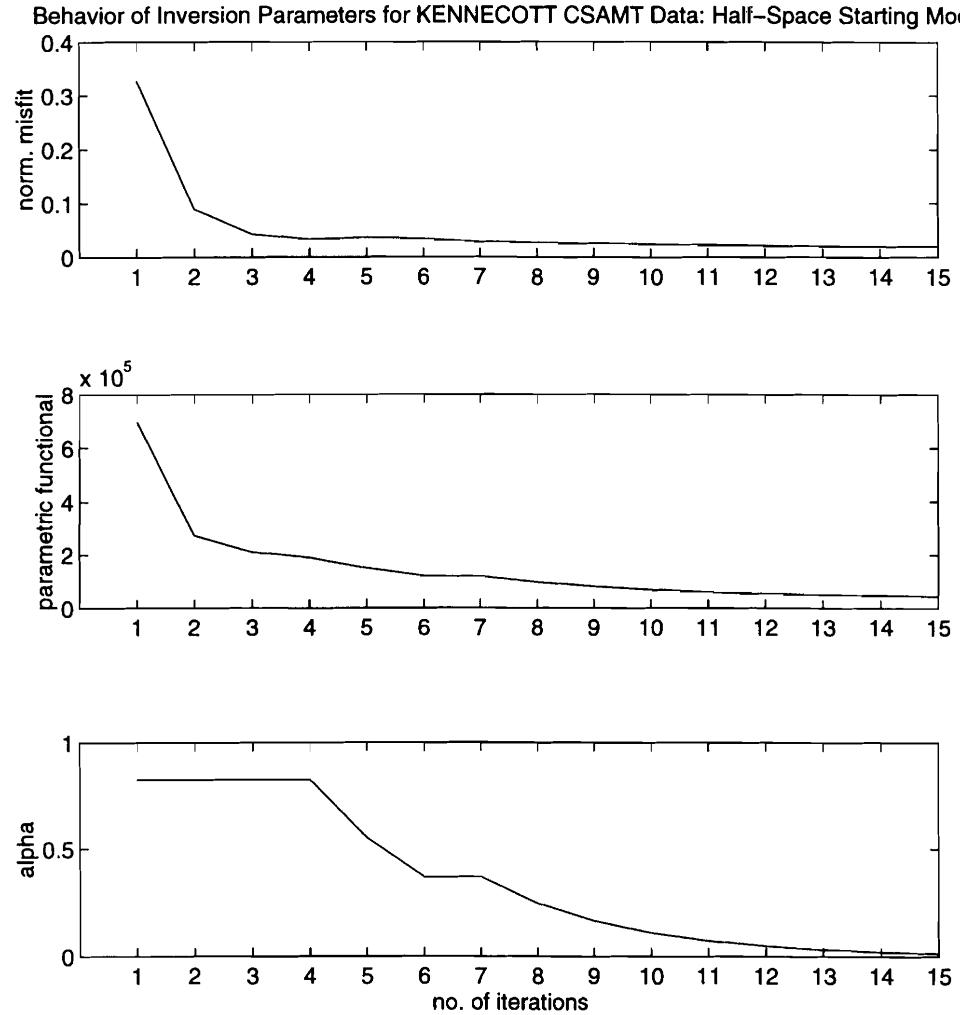

Fig. 19. Behavior of normalized misfit, parametric functional and regularization parameter (α) for TM mode inversion of Kennecott Exploration CSAMT data Exploration utilizing a 100 $\Omega{\cdot}$m half-space as starting model.

Appendix: The Regularized Conjugate Gradient Method

This method uses the same ideas as the conventional conjugate gradient method. However, the iteration process is based on the calculation of the regularized steepest descent directions. The theory presented here follows that of Zhdanov (1993).

To obtain a stable solution for the inverse problem, we minimize the parametric functional of Eq. (22):

$$P^{\alpha}(m,d) = \|\hat{W}_d A(m) - \hat{W}_d d\|^2 + \alpha S(m) = minimum \tag{A.1}$$

where d are the observed data, m is the unknown model, $A(m)$ is the operator of forward modeling, $\hat{W}_d$ is the data weighting matrix and $S(m)$ is the stabilizing functional. If we suppose that the space of data D is a Hilbert space with some given metric and the space of models M is also a

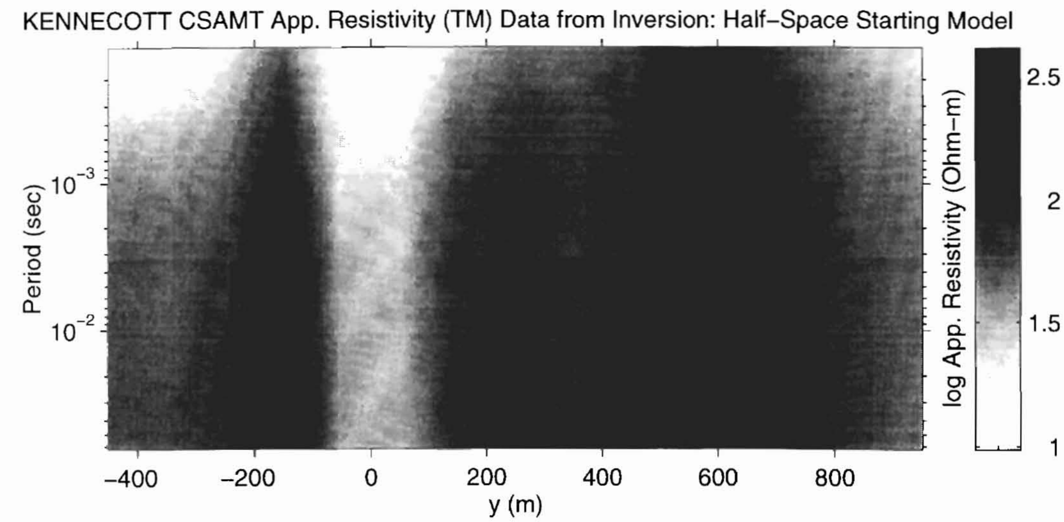

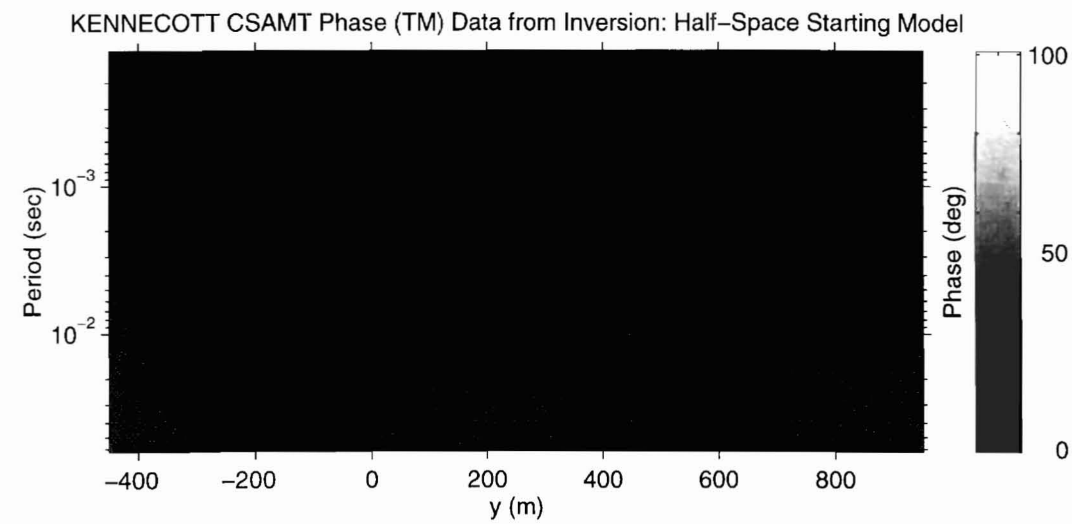

Fig. 20. Pseudosections of apparent resistivity and phase CSAMT data resulting from TM mode 2-D inversion of Kennecott Exploration data utilizing a 100 Ω·m half-space as starting model.

Hilbert space with another metric, then:

$$P^{\alpha}(m,d) = (W_d A(m) - W_d d, W_d A(m) - W_d d)_D + \alpha(m - m_{apr}, m - m_{apr})_M \tag{A.2}$$

where m_{apr} is some *a priori* given model. To solve the problem of minimization (A.1) we have to calculate the first variation with respect to m:

$$\begin{aligned} \delta P^{\alpha}(m,d) &= \delta(W_d A(m) - W_d d, W_d A(m) - W_d d)_D + \alpha\delta(m - m_{apr}, m - m_{apr})_M \\ &= 2W_d^2(\delta A(m), A(m) - d) + 2\alpha(\delta m, m - m_{apr}). \end{aligned} \tag{A.3}$$

Taking into consideration that the operator A is differentiable

$$\delta A(m) = F_m \delta m \tag{A.4}$$

where F_m is a linear operator, the Frechet derivative of A, we obtain

$$\begin{aligned}\delta P^{\alpha}(m,d) &= 2W_d^2(F_m\delta m, A(m)-d)_D + 2\alpha(\delta m, m-m_{apr})_M \\ &= 2W_d^2(\delta m, F_m^*(A(m)-d)+\alpha(m-m_{apr}))\end{aligned} \tag{A.5}$$

where F_m^* is the adjoint operator of F_m.

In order to obtain a direction of descent at each iteration, we select

$$\delta m = -k^{\alpha} l^{\alpha}(m) \tag{A.6}$$

where k^{α} is some positive real number and $l^{\alpha}(m)$ is the direction of steepest ascent of the functional $P^{\alpha}(m,d)$:

$$l^{\alpha}(m) = F_m^* W_d^2(A(m)-d) + \alpha(m-m_{apr}). \tag{A.7}$$

By substituting Eqs. (A.6) and (A.7) into Eq. (A.5) we obtain

$$\delta P^{\alpha}(m,d) = -2k^{\alpha}(l^{\alpha}(m), l^{\alpha}(m)) < 0. \tag{A.8}$$

The iteration process for the regularized steepest descent is constructed as follows:

$$m_{n+1} = m_n + \delta m = m_n - k^{\alpha} l^{\alpha}(m). \tag{A.9}$$

The coefficient k^{α} is obtained by the minimization of the parametric functional $P^{\alpha}(m,d)$ with respect to k^{α}:

$$P^{\alpha}(m_{n+1},d) = P^{\alpha}(m_n - k_n^{\alpha} l^{\alpha}(m_n)) = min. \tag{A.10}$$

The iteration process for the regularized conjugate gradient method combines previous and current "directions" of ascent:

$$m_{n+1} = m_n + \delta m = m_n - k^{\alpha}\tilde{l}^{\alpha}(m). \tag{A.11}$$

On the first step, we use the "direction" of regularized steepest ascent:

$$\tilde{l}^{\alpha}(m_0) = l^{\alpha}(m_0).$$

On the next step, the "direction" of ascent is the linear combination of the regularized steepest ascent on this step and the "direction" of ascent $\tilde{l}^{\alpha}(m_0)$ on the previous step:

$$\tilde{l}^{\alpha}(m_1) = l^{\alpha}(m_1) + \beta_0^{\alpha}\tilde{l}^{\alpha}(m_0).$$

On the n^{th} step

$$\tilde{l}^{\alpha}(m_{n+1}) = l^{\alpha}(m_{n+1}) + \beta_n^{\alpha}\tilde{l}^{\alpha}(m_n). \tag{A.12}$$

The coefficients β_n^{α} are determined by the formula:

$$\beta_n^{\alpha} = \frac{\|l^{\alpha}(m_{n+1})\|^2}{\|l^{\alpha}(m_n)\|^2}. \tag{A.13}$$

REFERENCES

de Groot-Hedlin, C. D. and S. C. Constable, Occam's inversion to generate smooth, two-dimensional models from magnetotelluric data, *Geophysics*, **93**, 1613–1624, 1990.

de Lugão, P. P. and P. E. Wannamaker, Calculating the two-dimensional magnetotelluric Jacobian in finite elements using reciprocity, *Geophys. J. Int.*, **127**, 806–810, 1996.

Lapidus, L. and G. F. Pinder, *Numerical Solutions of Partial Differential Equations in Science and Engineering*, 677 pp., John Wiley and Sons, New York, 1982.

Rodi, W. L., A technique for improving the accuracy of finite element solutions for magnetotelluric data, *Geophys. J. R. Astr. Soc.*, **44**, 483–506, 1976.

Sasaki, Y., Two-dimensional joint inversion of magnetotelluric and dipole-dipole resistivity data, *Geophysics*, **54**, 254–262, 1989.

Smith, J. T. and J. R. Booker, Rapid inversion of two- and three-dimensional magnetotelluric data, *J. Geophys. Res.*, **96**, 3905–3922, 1991.

Tikhonov, A. N. and V. Y. Arsenin, *Solutions of Ill-Posed Problems*, 258 pp., John Wiley and Sons, New York, 1977.

Tripp, A. C., G. W. Hohmann, and C. M. Swift, Two-dimensional resistivity inversion, *Geophysics*, **49**, 1708–1717, 1984.

Wannamaker, P. E., J. A. Stodt, and L. Rijo, A stable finite element solution for two-dimensional magnetotelluric modeling, *Geophys. J. R. Astr. Soc.*, **88**, 277–296, 1987.

Zhdanov, M. S., Tutorial: regularization in inversion theory, Colorado School of Mines, 1993.

Zhdanov, M. S., N. G. Golubev, V. V. Spichak, and Iv. M. Varentsov, The construction of effective methods for electromagnetic modelling, *Geophys. J. R. Astr. Soc.*, **68**, 589–607, 1982.

Zhdanov, M. S., N. G. Golubev, V. V. Spichak, Iv. M. Varentsov, and V. A. Krylov, *The Methods for Electromagnetic Fields Modelling*, 200 pp., (COMMEMI project), Nauka, Moscow, 1990.